1967

Residual stress and the local buckling strength of steel columns, January 1967

F. Nishino

L. Tall

LEHIGH UNIVERSITY INSTITUTE OF RESEARCH

Welded and Rolled T-1 Columns

RESIDUAL STRESS AND LOCAL BUCKLING STRENGTH OF STEEL COLUMNS

by
Fumio Nishino
Lambert Tall

Fritz Engineering Laboratory Report No. 290.11

Welded Built-up and Rolled Heat-Treated T-1 Steel Columns

RESIDUAL STRESS AND LOCAL BUCKLING STRENGTH OF STEEL COLUMNS

by

Fumio Nishino

Lambert Tall

This work has been carried out as part of an investigation sponsored by the United States Steel Corporation.

Fritz Engineering Laboratory
Department of Civil Engineering
Lehigh University
Bethlehem, Pennsylvania

January 1967

Fritz Engineering Laboratory Report No. 290.11

TABLE OF CONTENTS

ABSTRACT

This report presents the results of a study of the local buckling strength of steel columns. The effect of residual stress is given attention. The finite difference method was employed throughout the analysis and proved to be a suitable method for obtaining solutions for this type of problem. Numerical results are presented for plate buckling curves for plates with idealized residual stress distributions of various magnitudes. The boundary conditions of the plates are simply supported at the loading edges, and four combinations of free, simply supported and fixed at the unloaded edges. A few illustrative results are also presented for the local buckling of column cross sections.

The theoretical results were correlated with experimental results of four pilot tests of square welded columns of ASTM A514 constructional alloy steel.

1. INTRODUCTION

The strength of steel columns has been investigated to a great extent and variety by many investigators [1] through [6], who introduced residual stresses as the main factor influencing the buckling strength of centrally loaded columns. As a rule, most of the cross sections of steel columns consist of plate elements. It is possible, therefore, that even before instability of a column takes place, the component plates may buckle locally so that a premature failure of the entire column will occur characterized by a distortion of the cross section.

Local buckling may be defined as the bifurcation of equilibrium of adjacent theoretically flat plates into distorted shapes in their own plane with the lines of intersection of the plates remaining straight. The efficient design of a column requires a cross section with comparatively thin plates, and so, local buckling may increase in significance as steels of higher yield point are used. Hence, consideration must be given to the stability of plate elements so that the most economical cross section can be designed.

The buckling load of plates is different from the ultimate load which the plates can carry, as opposed to a column for which the buckling load has been found to be of a similar magnitude to the ultimate load for practical columns. Plates may be able to sustain the buckled state

with ultimate loads considerably exceeding the buckling load. However, the difference between buckling and ultimate loads becomes significant only for very thin plates which is not the case for plate elements of structural steel columns. Once buckling occurs in plate elements of columns, the stiffness for axial compression of the plates reduces, and this in turn reduces the bending rigidity of the column, possibly leading to overall failure of the column. Hence, the buckling load of plate elements or plate assemblies is more important as a guide for the design of column cross sections than in determining the ultimate load.

The local buckling of a steel column with thin component plates is considered in this report. The development of the theory of elastic buckling of thin plates is reviewed in References 7 and 8. Reference 7 includes an approximate solution of elastic local buckling problems in plate assemblies, together with a review of other investigations in the field. A solution of buckling of the plate assembly has been obtained by the energy method for elastic columns having I, Z, channel, and rectangular tube sections [9][10].

Attempts to extend the theory of plate stability into the inelastic range were made by many investigators in the early 30's[7][11][12]. However, a comprehensive theory of the inelastic buckling of plates has had to await the development of the theory of plasticity.

There are two main current trends in the development of inelastic buckling of plates, one based on Hencky's total strain or deformation theory[13] and the other on Prandtl-Reuss' incremental theory[14]. Bijlaard appears to have been the first to arrive at satisfactory theoretical solutions for inelastic buckling theories of plates[15][16][17]. His work is the most comprehensive of all available including those which appeared later. He considered both the incremental and the total strain theories and concluded that the total strain theory is correct since it leads to lower inelastic loads than are obtained from the incremental theory[18]. Ilyushin applied the total strain theory to derive the basic differential equation for the strain-reversal model[19], which was further modified to non-strain-reversal models by Stowell[20]. Handelman and Prager presented the inelastic buckling theory of plates based on the incremental theory of plasticity[21]. Pearson improved it by using Shanley's concept[22]. The assumptions of these theories are summarized in Table 1.

The total strain theory assumes a one-to-one correspondence between stress and strain in the inelastic range when the material is under load. The incremental theory, on the other hand, assumes a one-to-one correspondence between the rate of change of stress and the rate of change of strain. The important basic difference between these two theories lies in the fact that the stress-strain relationship is independent of the loading history in the total

strain theory. In the incremental theory, the stress depends on the manner in which the state of strain is obtained.

Although many discussions have been made, no definite conclusion on these theories of plasticity has yet been made[21] through [27]. It appears logical that the loading history must play a role, in general. It has been said, however, that for the special case of the buckling of materials such as aluminum, magnesium, titanium alloys and high-strength steels, the behavior is similar to that defined by the total strain theory[27]. Test results have further shown that only the total strain theory gives good agreement[17][20][28][29][30]. The assumptions which lead to the best agreement between theory and test data for the inelastic buckling of aluminum-alloy flat plates under compression are the stress and strain intensities defined by the octahedral-shear law and the total strain type stress-strain relationship applied to the plates, together with Shanley's concept[30]. In this report, both theories are used to determine the stiffness of the yielded portion of the plates.

The above theoretical studies and the experiments have been advanced mainly for aluminum plates. The plastic buckling theory of steel plates were developed in Ref. 31. In that study, the four independent instantaneous flexure and shear moduli of an orthotropic plate were

determined from the test results of the material under consideration.

The effect of residual stress on the elastic buckling strength of steel plates were studied and presented in Ref. 32, where a case of center welded plates was analyzed with the aid of integral equations; it was shown that the residual stresses could influence the elastic buckling strength of a plate. The analysis was further developed into the inelastic range, where it was shown that integral equations could be used to solve the inelastic buckling problem[29]. An analytical solution was obtained in Ref. 29 for simply supported, fixed and elastically restrained plates at the unloaded edges, together with a numerical solution for simply supported plates with a particular distribution of residual stress.

A column cross section consists of a few plate elements. Since the plate elements are connected to each other, a complete analysis of local buckling must be made for the plate assembly as a unit. If an individual analysis is made for each plate element, the restrictions at the unloaded edges of each plate must be determined. However, if such individual analyses are made on plate elements for several combinations of particular edge condition, such as: free, simply supported and fixed, the results may be useful in estimating the overall buckling strength of the cross section. Hence, the study covered in this report

includes the analysis of plate elements and the analyses of plate assemblies.

The local failure of plate elements of a column is a particular case of plate instability in which the plates can be considered as simply supported at the two opposite loading edges on which the distributed thrust is applied. The other two edges are free of loading and the supporting conditions would be, in general, either fixed for translation and elastictically restrained for rotation, or else free. Since exact solutions can be made for most of the cross sections of structural columns, the following analysis considers only special boundary conditions at the unloaded edges to obtain buckling solutions for plate elements. These are the combinations of free, simply supported and fixed at the unloaded edges.

At the two opposite loading edges the boundary conditions for the local buckling of cross sections are the same as for the plate elements, namely, simply supported. The boundaries at the other two edges of the plate elements are either free, when the edge does not meet with the other plate, or elastically restrained for rotation when the edge intersects with the other plates. Only rigid connections, which resemble joints in rolled shapes and welded intersections, are considered for the intersection. Particular attention is given to column cross sections of rectangular box-, H-, channel-, tee-, and angle-shapes.

When residual stresses exist, the stress in the plate cannot be considered as uniform. The plates may yield, partially, at a certain loading due to the existence of compressive residual stress; thereafter, the plate is no longer homogeneous. The tangent modulus concept is introduced for the buckling in this state of stress, namely, no strain reversal is assumed to occur at the instant of buckling[7].

The anlytical solutions are not feasible, in general, without a considerable amount of effort, consequently, approximate methods must be considered. The solutions are obtained by a finite difference approximation of differential equations. A digital computer was used to obtain numerical solutions.

2. ASSUMPTIONS

In addition to the usual assumptions for the analyses of thin plates[7][8] and to the assumption that no strain reversal takes place at the instant of buckling, the following specified conditions are implied in the analyses of this study:

Specified Conditions

(1) The thrust is at the two opposite edges of the plate element in the middle plane, when the plate is simply supported. The strain distribution due to the thrust is uniform in the direction of the thrust and changes linearly in the direction perpendicular to the thrust.

(2) The boundary conditions at the two edges where no loading is applied, are either free, simply supported or fixed if no plate intersects; the boundary at the intersection of component plates is considered as rigidly connected where the line of intersection remains straight.

(3) The plate thickness and material properties are constant in the same direction as the application of thrust.

(4) The residual stress is present only along the same directions as the thrust and its magnitude is constant in that direction.

(5) The wave length of buckling is identical on each plate element in a buckled plate assembly, and there is

no phase lag between plates.

Further, the following assumptions are made in obtaining numerical solutions:

(1) The stress-strain relationship of uniaxially loaded steel is elastic-perfectly-plastic.

(2) The plate thickness is constant in the plate element.

(3) The residual stress distribution is symmetric if any symmetric axis is present in the plate element or in the plate assembly.

(4) Poisson's ratio in the elastic range is 0.3.

(5) The residual stress varies linearly inside the cell; deflections are known at the centers of mesh cells in the analysis by the finite difference approximation.

Some additional assumptions are necessary with the progress of the analyses and they will be discussed when they appear.

The coordinate systems for plate elements and for plate assemblies are shown in Fig. 1. The coordinate x is perpendicular to the middle plane of the plate, y is normal to the thrust in the middle plane and z is the coordinate parallel to the thrust and to the residual stress. When a plate assembly is considered, a coordinate system is set to each plate and they are distinguished by subscript numbers.

3. ANAYLSIS OF PLATE BUCKLING

3.1 Stress-Strain Relationship and Basic Differential Equation

When a buckling problem is analyzed, the relationship between stress and strain must be defined both in the elastic and inelastic ranges of material. The most fundamental relationship of stress and strain is that obtained from a coupon test in uniaxial tension or compression. Figure 2a shows a typical stress-strain relationship for a strain hardening material. Figure 2b presents an idealized stress-strain relationship for steel, that of elastic-perfectly-plastic.

The stress-strain relationship by Bijlaard[15] is derived under the assumption that plastic deformations are governed by the elastic shearing energy of the octahedral type. By subtracting the initial stresses and strains before buckling from the total stresses and strains, the relationship between stress components and strain components due to buckling is obtained[15][16], where no strain reversal is considered. Denoting the normal stress components in the z and y direction by σ_z and σ_y and shear stress by τ, for buckling from a state of uniaxial compression (σ_z, σ_y = 0 and τ= 0) the relationship is given by the following equations

$$\delta\sigma_z = E(k_1\delta\epsilon_z + k_2\delta\epsilon_y)$$
$$\delta\sigma_y = E(k_2\delta\epsilon_z + k_3\delta\epsilon_y) \quad (1)$$
$$\delta\tau = Ek_4\delta\gamma$$

where k_1 to k_4 are defined as follows by Poisson's ratio ν, tangent modulus E_t on the stress-strain curve of the compression coupon at the stress intensity of σ_z, and by the secant modulus E_s, which is shown in Fig. 2.

$$k_1 = \frac{1+3\left(\frac{E_t}{E_s}\right)}{(5-4\nu+3e)-(1-2\nu)^2\left(\frac{E_t}{E}\right)}$$
$$k_2 = \frac{2-2(1-2\nu)\left(\frac{E_t}{E}\right)}{(5-4\nu+3e)-(1-2\nu)^2\left(\frac{E_t}{E}\right)}$$
$$k_3 = \frac{4}{(5-4\nu+3e)-(1-2\nu)^2\left(\frac{E_t}{E}\right)} \quad (2)$$
$$k_4 = \frac{1}{2+2\nu+3e}$$
$$e = \frac{E}{E_s} - 1$$

E is the modulus of elasticity, $\delta\sigma_z$, $\delta\sigma_y$, and $\delta\epsilon_z$, $\delta\epsilon_y$ are the stresses and strains due to the buckling of the plate in the z- and y-directions, respectively. Substitution of $E_s = E_t = E$ and e=0 into Eq. 2 changes the relationship of Eq. 1 to that in the elastic domain.

The relationship derived by Ilyushin[19] and by Stowell[20] with the assumption of Poisson's ratio being equal to 0.5 even in the elastic domain, can be obtained by substituting $\nu = 0.5$ into Eq. 2.

A loss of strain in the strain history, which is the main assumption of the incremental theory, amounts only to a neglect of the initial plastic deformation at the instant of buckling, which is taken into account by equating e, as defined by Eq. 2 (which is equal to the ratio of plastic strain to elastic strain, ϵ_p/ϵ_e) to zero. Equation 2 then becomes identical with the ones derived by Handelman and Prager[21]. With the stress-strain relationship, the bending and twisting moments, M_z, M_y, and M_{zy}, which exist in an element of a slightly buckled plate are shown by the following equations

$$M_z = -EI\left(k_1\frac{\partial^2 w}{\partial z^2} + k_2\frac{\partial^2 w}{\partial y^2}\right)$$

$$M_y = -EI\left(k_2\frac{\partial^2 w}{\partial z^2} + k_3\frac{\partial^2 w}{\partial y^2}\right) \qquad (3)$$

$$M_{2y} = -M_{y2} = 2EIk_4\frac{\partial^2 w}{\partial z\,\partial y}$$

in which I is the moment of inertia of the plate defined by its thickness t

$$I = \frac{t^3}{12} \qquad (4)$$

The differential equation of equilibrium of an element in a slightly bent plate is[8]

$$\frac{\partial^2 M_z}{\partial z^2} + 2\frac{\partial^2 M_{zy}}{\partial z\,\partial y} + \frac{\partial^2 M_y}{\partial y^2} = \pm\sigma_z\frac{\partial^2 w}{\partial z^2} \qquad (5)$$

Substitution of Eq. 3 into Eq. 5 results in the basic differential equation, Eq. 6, which is applicable both in the

elastic and in the inelastic domain of the plate.

$$E\left[\frac{\partial^2}{\partial z^2}\left(Ik_1\frac{\partial^2 w}{\partial z^2}+Ik_2\frac{\partial^2 w}{\partial y^2}\right)+4\frac{\partial^2}{\partial z\partial y}\left(Ik_4\frac{\partial^2 w}{\partial z\partial y}\right)\right.$$

$$\left.+\frac{\partial^2}{\partial y^2}\left(Ik_2\frac{\partial^2 w}{\partial z^2}+Ik_3\frac{\partial^2 w}{\partial y^2}\right)\right]+t\sigma_z\frac{\partial^2 w}{\partial z^2}=0 \qquad (6)$$

Equation 6 was derived by Bijlaard[15][16][17] for a plate. When a plate assembly is considered, an equation can be set up for each plate element forming the same number of simultaneous equations as the number of plate elements.

3.2 General Approach

The equation governing plate buckling is a fourth order partial differential equation with variable coefficients, as seen in Eq. 6, where the stress σ_z is a function of the residual strain distribution and the strain distribution due to thrust. Both of these strains are assumed to be constant along the z-direction; however, both of them change their intensities in the direction perpendicular to the thrust in the middle plane of the plate, and consequently, the stress intensity is a function of the coordinate y. Since k_1 through k_4 are functions of strain intensities, they are also variables in the y-direction and thus, functions of the coordinate y.

$$\sigma_z = \sigma_z(y)$$
$$k_i = k_i(y) \qquad i = 1, 2, 3, \text{and } 4 \tag{7}$$

The distribution of strains due to thrust in the column cross section can be approximated by a simple function for practical purposes, such that the distribution along the coordinate y is uniform or changes linearly. The distribution of residual strain varies considerably as presented in Refs. 4, 6, 33, 34, and 35. Hence, idealization could be made in several ways for analysis, such as those of a triangular or parabolic distribution or a combination of broken straight lines. It would be evident, therefore, that a rigorous solution of the present problem is a quite difficult task.

Several approximate methods to obtain an eigenvalue have been developed for the cases where exact solutions are not obtainable or for the cases where they are quite difficult to obtain. They are summarized and discussed in Refs. 7 and 8. Among the methods, the finite difference method with the help of a high speed computer affords a powerful tool for the solution of the many problems involving ordinary and partial differential equation. The method has first been suggested by Richardson[36] for the determination of the eigenvalue, investigated independently by Collatz[37] and it was presented in a very broad and clear manner by Salvadori[38][39] with examples of the buckling of columns and plates.

The governing equation can be solved as it is by the finite difference method; however, if the deflected shape can be expressed as a product function of which one term is a simple known function, the problem can be reduced to an ordinary differential equation. The solution of the ordinary differential equation by the finite difference method is obtained much simpler and with less involved numerical computations. In the subsequent analysis, the deflected shape of the plate is assumed by the following product function which satisfies the boundary conditions at the loading edges

$$w = Y \sin \frac{p\pi}{L} z \qquad (8)$$

where Y is a function of the coordinate y alone and p is the number of half waves in the z-direction. This assumed shape is known to be the exact deflected shape for an elastic plate free of residual stress and the shape has been presumed as satisfactory by many investigators[15][19][20][21] for the plastic-buckling of a plate. It is known that the lowest buckling stress can be obtained by considering a plate buckling into a half wave in the z-direction; thus, it is necessary to consider only p equal to 1. Substituting Eq. 8 into Eq. 6, the basic differential equation can be shown finally in the following form, where the equation is divided by a constant I_o

$$\frac{d^2}{dy^2}\left(\frac{I}{I_0}K_3\frac{d^2Y}{dy^2}-\frac{\pi^2}{L^2}\frac{I}{I_0}K_2Y\right)-4\frac{\pi^2}{L^2}\frac{d}{dy}\left(\frac{I}{I_0}K_4\frac{dY}{dy}\right)$$
$$-\frac{\pi^2}{L^2}\frac{I}{I_0}K_2\frac{d^2Y}{dy^2}+\frac{\pi^2}{L^2}\left(\frac{\pi^2}{L^2}\frac{I}{I_0}K_1-\frac{t\sigma_z}{EI_0}\right)Y=0 \qquad (9)$$

3.3 Differential Equation and Boundary Conditions in Finite Differences

A finite difference analogue of a differential equation can be obtained directly from the given differential equation by replacing the derivatives with difference quotients. When the coefficients of the differential equation are not constant, average values replace the variable coefficients for the cells. It is necessary also to express the boundary conditions by finite differences in solving the difference equations.

The quotients which are used in the subsequent analysis can be found in most of the literature on numerical analysis, as, for example, in Refs. 38, 39, and 40. The first order central difference quotients are employed throughout the following analyses since the first order equations are easier to use than the higher order equations and the central differences are more accurate compared with backward or forward difference, and are particularly useful in the solution of boundary value problems[39].

The basic difference equation for an evenly spaced

mesh is derived by replacing the derivatives of Eq. 9 by the corresponding difference quotients. Thus, the equation at a mesh point is derived as follows showing the relationship of the deflections at five nearby mesh points

$$C_{1,i}Y_{i+2} + C_{2,i}Y_{i+1} + (C_{3,i} - C_{6,i})Y_i + C_{4,i}Y_{i-1} + C_{5,i}Y_{i-1} + C_{5,i}Y_{i-2} = 0 \tag{10}$$

where subscript i of the coefficients C shows that it is for the equation at mesh point i and subscript to the function Y denotes the deflection at the points. These are shown in Fig. 3a. The coefficients are defined as:

$$\left.\begin{aligned}
C_{1,i} &= \frac{I_{i+1}}{I_0} K_{3,i+1} \\
C_{2,i} &= -2\left(\frac{I_{i+1}}{I_0}K_{3,i+1} + \frac{I_i}{I_0}K_{3,i}\right) - \frac{\pi^2 r^2}{L^2}\left(\frac{I_{i+1}}{I_0}K_{2,i+1} + \frac{I_i}{I_0}K_{2,i} + 4\frac{I_{i+\frac{1}{2}}}{I_0}K_{4,i+\frac{1}{2}}\right) \\
C_{3,i} &= \frac{I_{i+1}}{I_0}K_{3,i+1} + 4\frac{I_i}{I_0}K_{3,i} + \frac{I_{i-1}}{I_0}K_{3,i-1} \\
&\quad + \frac{\pi^2 r^2}{L^2}\left(4\frac{I_i}{I_0}K_{3,i} + 4\frac{I_{i+\frac{1}{2}}}{I_0}K_{4,i+\frac{1}{2}} + 4\frac{I_{i-\frac{1}{2}}}{I_0}K_{4,i-\frac{1}{2}} + \frac{\pi^2 r^2}{L^2}K_{1,i}\right) \\
C_{4,i} &= -2\left(\frac{I_{i-1}}{I_0}K_{3,i-1} + \frac{I_i}{I_0}K_{3,i}\right) - \frac{\pi^2 r^2}{L^2}\left(\frac{I_{i-1}}{I_0}K_{2,i-1} + \frac{I_i}{I_0}K_{2,i} + 4\frac{I_{i-\frac{1}{2}}}{I_0}K_{4,i-\frac{1}{2}}\right) \\
C_{5,i} &= \frac{I_{i-1}}{I_0}K_{3,i-1} \\
C_{6,i} &= \frac{\pi^2 r^2}{L^2}\frac{t\sigma_z}{EI_0}r^2
\end{aligned}\right\} \tag{11}$$

where r is the distance between mesh cells. In the above definitions, the subscripts indicate that the coefficients with subscripts are the average values at the mesh points or at the middle of the mesh points. If the properties are not given at the middle of the mesh points, they have to be approximated from the properties of the neighboring mesh points.

It is noted that the k's are a function of loading and residual strains and that the term $\pi^2 r^2/L^2$ is a function of the aspect ratio of the plate and width of mesh points; thus $C_{6,i}$ is the only term including the width-thickness ratio. Noting that the width of the mesh points is equal to the plate width b divided by the number of cells, n, the term is rewritten

$$C_{6,i} = \frac{12\pi^2}{n^4}\left(\frac{b}{L}\right)^2\left(\frac{\sigma_{z,i}}{\sigma_Y}\right)\left(\frac{b}{t}\sqrt{\frac{\sigma_Y}{E}}\right)^2 \qquad (12)$$

The last term is the square of the non-dimensionalized width-thickness ratio, λ.

$$\lambda = \frac{12\pi^2}{n^4}\left(\frac{b}{L}\right)^2\left(\frac{\sigma_{z,i}}{\sigma_Y}\right) \qquad (13)$$

Introducing a new coefficient C_i, defined as

$$C_i = \frac{12\pi^2}{n^4}\left(\frac{b}{L}\right)^2\left(\frac{\sigma_{z,i}}{\sigma_Y}\right) \qquad (14)$$

the difference equation is written as

$$C_{1,i} Y_{i+2} + C_{2,i} Y_{i+1} + C_{3,i} Y_i + C_{4,i} Y_{i-1} + C_{5,i} Y_{i-2} = C_i \lambda^2 Y_i \qquad (15)$$

When the spacing is not equal as shown in Fig. 3b, the coefficients of the difference equations are different from Eq. 11 at mesh points, i+1, i and i-1. They are summarized in Appendix A.

Boundary Conditions

It is customary and convenient to end the plate on a mesh point (an "integer" station) or at the middle of mesh points (a "half-integer" station).

The boundary conditions for fixed, simply supported and free ends and at a point of symmetry are similarly obtained by replacing the expressions of boundary conditions by finite difference quotients and are summarized below. It is assumed that the plate thickness is constant near the boundaries. For boundaries on an integer station, i:

(1) Fixed

$$Y_i = 0 \qquad Y_{i+1} = Y_{i-1} \qquad (16)$$

(2) Simply supported

$$Y_i = 0 \qquad Y_{i+1} = -Y_{i-1} \qquad (17)$$

(3) Free

$$Y_{i+1} = \left(2 + \frac{\pi^2 r^2}{L^2} \frac{K_{2,i}}{K_{3,i}}\right) Y_i - Y_{i-1}$$

$$Y_{i+2}=\frac{1}{k_{3,i+1}}\left\{\left[\left(k_{3,i+1}+\frac{\pi^2\gamma^2}{L^2}k_{2,i+1}+\frac{\pi^2\gamma^2}{L^2}k_{4,i}\right)\left(2+\frac{\pi^2\gamma^2}{L^2}\frac{k_{2,i}}{k_{3,i}}\right)-\left(k_{3,i+1}-k_{3,i}\right)\right]Y_i-\left[\left(2k_{3,i+1}+\frac{\pi^2\gamma^2}{L^2}k_{2,i+1}+\frac{\pi^2\gamma^2}{L^2}k_{4,i}\right)+\left(2k_{3,i-1}+\frac{\pi^2\gamma^2}{L^2}k_{2,i-1}+\frac{\pi^2\gamma^2}{L^2}k_{4,i}\right)\right]Y_{i-1}+k_{3,i}Y_{i-2}\right\} \quad (18)$$

where $k_{2,i+1}$ and $k_{3,i+1}$ or $k_{2,i-1}$, and $k_{3,i-1}$ are the material properties outside the plate and, consequently, they must be assumed by the values within the plate. Linear extrapolation may be used, thus

$$\left.\begin{aligned} k_{2,i+1}&=2k_{2,i}-k_{2,i-1}\\ k_{3,i+1}&=2k_{3,i}-k_{3,i-1}\end{aligned}\right\} \quad (19)$$

(4) <u>At point of symmetry</u>

$$Y_{i+1}=Y_{i-1}\ ,\quad Y_{i+2}=Y_{i-2} \quad (20)$$

For boundaries on a half-integer station i + 1/2.

(1) <u>Fixed</u>

$$Y_i=Y_{i+1}=0 \quad (21)$$

(2) <u>Simply supported</u>

$$Y_{i+1}=-Y_i\ ,\quad Y_{i+2}=-Y_{i-1} \quad (22)$$

(3) Free

$$\left.\begin{aligned} Y_{i+1} &= \frac{-\left(K_{3,i+1}\frac{K_{2,i+\frac{1}{2}}}{K_{3,i+\frac{1}{2}}} + K_{2,i+1} - 4K_{4,i+\frac{1}{2}}\right)Y_i + 2\frac{L^2}{\pi^2\gamma^2}K_{3,i+\frac{1}{2}}\,Y_{i-1}}{K_{3,i+1}\frac{K_{2,i+\frac{1}{2}}}{K_{3,i+\frac{1}{2}}} - K_{2,i+1} - 4K_{4,i+\frac{1}{2}}} \\ Y_{i+2} &= \left(1+\frac{K_{2,i+\frac{1}{2}}}{K_{3,i+\frac{1}{2}}}\frac{\pi^2\gamma^2}{L^2}\right)\left(1-\frac{\frac{K_{2,i+\frac{1}{2}}}{K_{3,i+\frac{1}{2}}} + K_{2,i+1} + 4K_{4,i+\frac{1}{2}}}{K_{3,i+1}\frac{K_{2,i+\frac{1}{2}}}{K_{3,i+\frac{1}{2}}} - K_{2,i+1} - 4K_{4,i+\frac{1}{2}}}\right)Y_i \\ &\quad - \left[1 + \frac{2K_{3,i+\frac{1}{2}}\left(1+\frac{K_{2,i+\frac{1}{2}}}{K_{3,i+\frac{1}{2}}}\right)}{K_{3,i+1}\frac{K_{2,i+\frac{1}{2}}}{K_{3,i+\frac{1}{2}}} - K_{2,i+1} - 4K_{4,i+\frac{1}{2}}}\right]Y_{i-1} \end{aligned}\right\} \quad (23)$$

(4) At point of symmetry

$$Y_{i+1} = Y_i \quad , \quad Y_{i+2} = Y_{i-1} \qquad (24)$$

The boundary conditions at the intersection of plates and compatibility of slope and equilibrium of moment can be obtained in finite difference forms by replacing the derivatives in their expressions. However, instead of simply transferring the conditions for the differential equation into the difference forms, a different approach can be made. Consider the folded plate as if it is a continuous plate simply supported at the intersection. Then the whole plate can be solved as a single plate with such internal restraints that the deflections are zero at the intersections. The zero

deflection implies that the lateral force is in equilibrium with the reaction at the point, regardless of its value. The basic difference equation at a mesh point is the equilibrium equation of lateral force; zero deflection, in turn, implies that no difference equation is to be considered at the point. Thus, if an angle cross section is considered as shown in Fig. 4 as an example, the difference equations are set up at all mesh points except at point 6, and consequently the problem results in 9 simultaneous equations with proper boundary conditions at edges 1 and 10.

The difference equations at mesh points 4, 5, 7, and 8 become those as follows, since the deflection Y is equal to zero at mesh point 6.

$$\left.\begin{aligned}
C_{2,4}Y_5 + C_{3,4}Y_4 + C_{4,4}Y_3 + C_{5,4}Y_2 &= C_4\lambda^2 Y_4 && \text{at mesh point 4}\\
C_{1,5}Y_7 + C_{3,5}Y_5 + C_{4,5}Y_4 + C_{5,5}Y_3 &= C_5\lambda^2 Y_5 && \text{at mesh point 5}\\
C_{1,7}Y_9 + C_{2,7}Y_8 + C_{3,7}Y_7 + C_{5,7}Y_5 &= C_7\lambda^2 Y_7 && \text{at mesh point 7}\\
C_{1,8}Y_{10} + C_{2,8}Y_9 + C_{3,8}Y_8 + C_{4,8}Y_7 &= C_8\lambda^2 Y_8 && \text{at mesh point 8}
\end{aligned}\right\} \quad (25)$$

When tee- and H-sections are considered, three plates intersect at a point. In this case, consider half of a flange, of which the flexural rigidity and the thickness are twice as large as actual, because of the symmetry of the shape. Then, the analysis is the same as for an intersection where only two plates intersect.

Averaging

When local buckling of columns is considered, the stress intensity in the component plates is not uniform. This is partially due to the existence of residual stress and partly due to the nonuniform external thrust, which arises due to the bending of the column prior to local buckling. The finite difference method of solving differential equations can be interpreted as solving a discrete physical system whose properties are uniform within the unit and whose response approximates that of continuous plates. New assumptions must be made concerning this averaging.

It is assumed that the eigenvalue of the set of basic difference equations, Eq. 15, is proportional to the coefficient, $C_i^{\ 2}$, which includes the term to be determined, and proportional to the reciprocal of the other coefficients. This is an assumption extended by a knowledge of the buckling of uniform columns where the differential equation is

$$EI \frac{d^4u}{dz^4} + A\sigma_{cr} \frac{d^2u}{dz^2} = 0 \qquad (26)$$

and the eigenvalue is shown[8] to be proportional to $A\sigma_{cr}/EI$, where σ_{cr} is the term to be determined.

Based on the above assumption, the averaging of the stress and material and geometric properties is accomplished as follows:

$$\left.\begin{aligned} \sigma_{z,i} &= \frac{1}{\Delta y_i}\int_0^{\Delta y_i} \sigma_z \, dy \\ \frac{1}{I_i} &= \frac{1}{\Delta y_i}\int_0^{\Delta y_i} \frac{1}{I} \, dy \\ \frac{1}{k_{j,i}} &= \frac{1}{\Delta y_i}\int_0^{\Delta y_i} \frac{1}{k_j} \, dy \quad , \quad j = 1, 2, 3 \text{ and } 4 \end{aligned}\right\} \qquad (27)$$

The above averaging method for stress intensity and flexural rigidity follows from the physical meaning of them. The averaging method of the k's is not straightforward, however; they are constant in the elastic range and even in the inelastic range where they are variable. No significant difference of numerical value is possible from their definition. Thus, the method of averaging for these variables may not be important. This assumption can be justified from the fact that it is made in order to obtain accurate results as far as possible with the smallest amount of labor, and from the fact that, if a closer mesh is used, the averaging method will lose its significance for engineering problems.

4. PROCEDURE OF NUMERICAL COMPUTATION

For the buckling analysis of a partially yielded plate, the distribution of stress and the stiffness of the material are a function of the loading and of the residual stress distribution so that it is easier to solve for a critical width-thickness ratio under a known loading rather than for a critical load on a plate with known geometry.

4.1 Formation of Matrix Equation

The geometric shape of a plate or a plate assembly must be fixed, for which the analysis will be made. Since the analysis is made for the critical width-thickness ratio under a given strain and consequently under a given loading, the thickness of the plate is yet to be determined. When a plate assembly is considered it is necessary that the relationship of the thickness among plate elements is given so that when a width-thickness ratio of an element is determined, the rest will be determined automatically. Then specifying the number of mesh points and giving the magnitude of residual strains and strains due to thrust at the edges of the plates and at all edges of the mesh cells, the concentrated stress intensity may be computed at each mesh point, as well as the average moduli of the plates (k_1 through k_4), and rigidity, I, at each mesh cell and the loading, of which details are given in Appendix B. With

matrix equation[39][41][42][43]. Preference is given to a method which leads to accurate results with the least amount of computation. Two procedures are considered; a trial method with which one seeks to find λ^2 by trial and error, substituting a guessed value into Eq. 29 and evaluating the determinant; and an iterative method which converges to the largest eigenvalue and at the same time gives the corresponding eigenvector when the form of the matrix equation is as follows,

$$\mathbb{H}\ \mathbb{X} = \lambda^2 \mathbb{X} \tag{30}$$

where H is a square matrix. It is necessary to change Eq. 29 into the above form prior to applying the iterative method. Computing the inverse of the $\mathbb{A}$-matrix and multiplying it on both sides of the equation, Eq. 28 becomes as follows.

$$(\mathbb{A}^{-1}\mathbb{B})\,X = \frac{1}{\lambda^2}X \tag{31}$$

Considering ($\mathbb{A}^{-1}$ $\mathbb{B}$) as $\mathbb{H}$, it is obvious that the procedure results in the largest root of $\frac{1}{\lambda^2}$ and consequently in the smallest value of λ^2 and the corresponding eigenvector. A brief comparison of the two methods for this particular problem are given in Appendix C.

4.3 Plate Buckling Curve

The critical width-thickness ratio is a function of the aspect ratio of the plate as well as of the loading,

when the mechanical properties, width of the plate and residual stress distribution are fixed. Usually the structural column is long enough, so that local buckling takes place in such wave lengths that the aspect ratio of the buckled plate in half wave lengths corresponds to the ratio which gives the minimum width-thickness ratio[7].

Repeating the analysis described in the previous article for different lengths of the plate, the relationship between the width-thickness ratio and the aspect ratio under a constant loading is obtained, from which the minimum width-thickness ratio and the corresponding aspect ratio and thus the half wave length of local buckling, are determined. The computational schemes are given in Fig. 5 for both the iterative and the trial methods, to obtain the relationship between aspect ratio and width-thickness ratio. Although it is possible to determine the minimum width-thickness ratio and the corresponding aspect ratio by plotting the results, an additional scheme is considered in such a way that the computer seeks the aspect ratio and determines the minimum width-thickness ratio. Repeating the computation on several different loadings, the results can be plotted as they are for the plate buckling curves of stress versus the minimum critical width-thickness ratio relationship.

It is well known that when only the length of a buckling plate is changed, the corresponding critical width-thickness ratio is infinite for the infinitesimally

short plate, then it will decrease and reach the minimum value for a certain length which is sought, thereafter it will increase monotonically with the increasing length.[7] As a special case of the curves, a plate simply supported and free at the unloaded edges has no minimum width-thickness ratio, instead it decreases monotonically with increase of the length and is asymptotic to the extreme value.[7] The local buckling of plate assemblies responds to the change of the local buckling length in a manner similar to that of the buckling of a plate element. Any relationship which resembles the above relationship can be used to seek the aspect ratio numerically. The following relationship between the width-thickness ratio and the aspect ratio may be assumed for numerical computation.

$$\lambda = C_1\left(\frac{b}{L}\right)^2 + C_2\left(\frac{L}{b}\right)^2 + C_3 \tag{32}$$

where C_1, C_2, and C_3 are constants. Knowing three points which are on the λ versus L/b curve, the constant can be determined. Then the aspect ratio, for which λ is the minimum, can be obtained by differentiating λ with respect to L/b and equating it to zero. Thus,

$$\frac{d\lambda}{d\left(\frac{L}{b}\right)} = -2C_1\left(\frac{L}{b}\right)^{-3} + 2C_2\left(\frac{L}{b}\right) = 0 \tag{33}$$

and the aspect ratio sought is obtained from

$$\frac{L}{b} = \sqrt[4]{\frac{C_1}{C_2}} \tag{34}$$

The known three points are

$$\left(\lambda_1, \frac{L_1}{b}\right), \left(\lambda_2, \frac{L_2}{b}\right) \text{ and } \left(\lambda_3, \frac{L_3}{b}\right)$$

and finally, the aspect ratio is computed from

$$\frac{L}{b} = \frac{1}{b^2}\sqrt{\frac{L_1^2\lambda_3 + L_2^2\lambda_1 + L_3^2\lambda_2 - L_1^2\lambda_2 - L_2^2\lambda_3 - L_3^2\lambda_1}{\frac{\lambda_2}{L_1^2} + \frac{\lambda_3}{L_2^2} + \frac{\lambda_1}{L_3^2} - \frac{\lambda_3}{L_1^2} - \frac{\lambda_1}{L_2^2} - \frac{\lambda_2}{L_3^2}}} \qquad (35)$$

With this aspect ratio, the corresponding width-thickness ratio which must be compared with the known values of λ_1, λ_2, and λ_3, may be computed. Since the relationship of Eq. 32 may be close to the actual relationship (but not exactly true) and also due to the error involved in numerical computation, several trials are necessary to find out the true value of the aspect ratio and thus the minimum critical width-thickness ratio. The scheme for this procedure is shown in Fig. 6 with the iterative method of finding the eigenvalue.

5. NUMERICAL RESULTS

In Chapter 2, the material properties are specified to resemble steel so that the following numerical results are applicable only to steel plates.

The effect of residual stress on the buckling strength of the plates is the main purpose of this study. Idealized patterns of residual stress distributions are considered as shown in Fig. 7. The triangular distribution as shown in Figs. 7a and 7b resembles the patterns found in the flange and web on rolled wide-flange shapes in which the magnitudes of the maximum compressive and tensile residual stresses are assumed to be the same. The patterns shown in Figs. 7c and 7d resemble the patterns found in welded built-up shapes. The tensile residual stress of the weld is assumed to be equal to the yield stress of the parent material at the weld. (The tensile residual stresses at the weld in actual welded plates are higher than the yield stress of the parent material for plates of structural carbon steel[33][34] and they are lower for plates of constructional alloy steel[35]. However, the tensile residual stress is distributed over only a small fraction of total area of the plates and the effect of the difference may be neglected.) The pattern of real residual stress distribution in rolled heat-treated shapes of T-1 steel is the closest to those of Figs. 7a and 7b among rolled shapes of structural steels[4][44].

The distributions of Figs. 7c and 7d are very close to the pattern found in welded T-1 plates.[35]

An error is inherent in finite difference solutions when the method is used as an approximate method for problems governed by a differential equation. In a engineering problem, it is not essential to have a solution of great accuracy. Instead, the aim was that the errors in the numerical results would not exceed two percent in any case; in most cases they were less than one percent. Somewhat generalized and detailed analyses and discussions of the errors of this particular problem are given in Ref. 45, on which this report is based.

5.1 Aspect Ratio and Critical Width-Thickness Ratio Relationship

It is important for the analysis of local buckling to find the minimum critical width-thickness ratio which is obtained when a plate of a particular aspect ratio is analyzed. Figure 8 shows the variation of the width-thickness ratio for the change of the aspect ratio of a buckling plate simply supported at the unloaded edges. Figure 8a is for a plate without residual stress, in which the minimum width-thickness ratio occurs at the aspect ratio of 1.0 for elastic buckling and at the aspect ratio of 0.7 for plastic buckling. A sudden jump of the aspect ratio, at which the width-thickness ratio is a nimimum, is noted between the elastic buckling and plastic buckling. This is because of an abrupt change of material

properties due to yielding of the material. A similar relationship for plates with residual stress distribution of welding type and cooling type are shown in Figs. 8b and 8c, respectively. The relationship for elastic buckling and plastic buckling are similar to those of plates free of residual stress. The sudden jump of the aspect ratio is observed between elastic buckling and elastic-plastic buckling of a plate with welding type residual stresses; the aspect ratio changes gradually with the increase of critical strain and approaches the value for plastic buckling. The jump is due again to the abrupt yielding over the large portion of the area of the plate. Since no abrupt yielding takes place in a plate with cooling type residual stresses, the change of the aspect ratio for the minimum critical width-thickness ratio is gradual from the value of elastic buckling to that of plastic buckling with increase of the critical strains.

The relationships between the critical width-thickness ratio and the aspect ratio for plates fixed at both of the unloaded edges and for plates fixed and free is similar to the relationship for simply supported plates. Figures 9 and 10 show the relationship for these plates. A plate simply supported and free at the unloaded edges does not have a mimumum critical width-thickness ratio; instead, there is an asymptote to a limiting value with increase of the aspect ratio of the buckling plate, as

shown in Fig. 11.

It should be noted that the above figures are results based on the total strain theory of plasticity. The incremental theory of plasticity results in a relationship similar to these figures for elastic-plastic buckling and in an identical relationship for plastic buckling with the plates free of residual stress and buckled right at the completion of full yielding.

5.2 Plate Buckling Curve

The minimum critical width-thickness ratio is a function of the critical strain and in turn a function of the critical stress, and hence the ratio is determined for a given critical strain or for a given stress. The relationship between the critical stress and the minimum critical width-thickness ratio was computed for plates with residual stresses. The residual stress patterns of Figs. 7b and 7d are assumed for plates both simply supported and fixed at the unloaded edges so as to resemble the component plates of box-section and web plates for wide-flange and channel-sections. Half of the residual stress patterns of Figs. 7a and 7c are assumed for plates free at one unloaded edge and fixed and simply supported at the other edge so as to resemble outstanding flanges of column cross sections. The complete results are shown in Figs. 12 through 15, where the figures are for the ratio of average critical stress to the static yield stress versus the non-dimensionalized

width-thickness ratio. The results are based on the total strain theory of plasticity unless otherwise noted.

The assumed residual stress patterns reduce the buckling strength in all cases considered. The reduction in the elastic buckling strength is rather constant for a residual stress pattern regardless of the width-thickness ratio of the plate, while the reduction in elastic-plastic buckling depends largely on the width-thickness ratio. The sudden jump of the plate buckling curve for plates with welding type residual stress is due to the penetration of yielding over a large portion of area at the same instant.

A critical value of width-thickness ratio exists in all cases considered; plates with width-thickness ratio less than this critical value sustain full yielding loads. The critical value depends on the magnitude of residual stress for the assumed residual stress distribution of the cooling type, whereas it is constant for practical purposes for the assumed residual stress patterns of the welding type.

5.3 Reduction Factor of Width-Thickness Ratio

Of practical interest in designing the component plates of columns is the width-thickness ratio with which the maximum load of a column can be sustained without any local failure; or, stated differently to find the ratio for which no local instability takes

place until the yield load of the cross section is reached. For this purpose, a reduction factor of the width-thickness ratio is introduced, which incorporates all effects due to the existence of residual stress. The critical width-thickness ratio of a plate with residual stresses can be expressed as follows with a reduction factor R and with the width-thickness ratio of the same plate free of residual stress

$$\left(\frac{b}{t}\right)_{\sigma_r} = R \cdot \left(\frac{b}{t}\right)_{\sigma_r=0} \tag{36}$$

where the subscript σ_r refers to the width-thickness ratio for a plate with residual stress and the subscript $\sigma_r = 0$ refers to a plate free of residual stress. Multiplying both sides of Eq. 36 with a factor $\sqrt{\epsilon_y}$ the non-dimensionalized relationship was obtained as follows

$$\lambda_{\sigma_r} = R \cdot \lambda_{\sigma_r=0} \tag{37}$$

The reduction factors were obtained from the plate buckling curves, Figs. 12 through 15, for critical stresses of 90, 95, and 100 percent of yield stress and they are plotted against the maximum magnitude of compressive residual stress in Figs. 16 through 19.

5.4 Numerical Results For Column Sections

Numerical results of the local buckling analysis on column cross sections can be obtained in a form similar to the plate buckling curve. However, the fact that there

place until the yield load of the cross section is reached. For this purpose, a reduction factor of the width-thickness ratio is introduced, which incorporates all effects due to the existence of residual stress. The critical width-thickness ratio of a plate with residual stresses can be expressed as follows with a reduction factor R and with the width-thickness ratio of the same plate free of residual stress

$$\left(\frac{b}{t}\right)_{\sigma_r} = R \cdot \left(\frac{b}{t}\right)_{\sigma_r=0} \tag{36}$$

where the subscript σ_r refers to the width-thickness ratio for a plate with residual stress and the subscript $\sigma_r = 0$ refers to a plate free of residual stress. Multiplying both sides of Eq. 36 with a factor $\sqrt{\epsilon_y}$ the non-dimensionalized relationship was obtained as follows

$$\lambda_{\sigma_r} = R \cdot \lambda_{\sigma_r=0} \tag{37}$$

The reduction factors were obtained from the plate buckling curves, Figs. 12 through 15, for critical stresses of 90, 95, and 100 percent of yield stress and they are plotted against the maximum magnitude of compressive residual stress in Figs. 16 through 19.

5.4 Numerical Results For Column Sections

Numerical results of the local buckling analysis on column cross sections can be obtained in a form similar to the plate buckling curve. However, the fact that there

are so many factors such as geometric shape, residual stress distribution and the stress at which the section buckles, on which the critical width-thickness ratio depends, makes it quite difficult to prepare curves which cover a wide variety of column cross sections with various patterns of residual stress distributions. Instead, numerical results were obtained for a few cases to illustrate the effect of residual stresses. Box- and H- sections were selected with idealized residual stress patterns of the welding type as shown in Figs. 20, and 21. The assumed patterns are more severe for local buckling strength than the residual stress distribution found in medium size welded built-up shapes* of T-1 steel** and are somewhat conservative when compared to those found in similar shapes of structural carbon steel. Thus, the patterns are not intended to predict the strength of any real column, but are only for demonstration and comparison purposes.

The analysis is made such that the minimum critical width-thickness ratio of the flange plate is obtained as a solution in non-dimensionalized form, with the given ratio between the widths of the web and the flange, b_w/b_f and with the given ratio between the thicknesses, t_w/t_f,

$$\lambda_f = \frac{b_f}{t_f}\sqrt{\frac{\sigma_Y}{E}} \qquad (38)$$

* "Medium size section" denotes in this study a cross section of which the component plates are roughly 6 to 12 inches in width and 1/4 to 1 inch in thickness.

** T-1 steel meets the requirements of ASTM A514 and/or A517 steel.

are so many factors such as geometric shape, residual stress distribution and the stress at which the section buckles, on which the critical width-thickness ratio depends, makes it quite difficult to prepare curves which cover a wide variety of column cross sections with various patterns of residual stress distributions. Instead, numerical results were obtained for a few cases to illustrate the effect of residual stresses. Box- and H- sections were selected with idealized residual stress patterns of the welding type as shown in Figs. 20, and 21. The assumed patterns are more severe for local buckling strength than the residual stress distribution found in medium size welded built-up shapes* of T-1 steel** and are somewhat conservative when compared to those found in similar shapes of structural carbon steel. Thus, the patterns are not intended to predict the strength of any real column, but are only for demonstration and comparison purposes.

The analysis is made such that the minimum critical width-thickness ratio of the flange plate is obtained as a solution in non-dimensionalized form, with the given ratio between the widths of the web and the flange, b_w/b_f and with the given ratio between the thicknesses, t_w/t_f,

$$\lambda_f = \frac{b_f}{t_f}\sqrt{\frac{\sigma_Y}{E}} \qquad (38)$$

* "Medium size section" denotes in this study a cross section of which the component plates are roughly 6 to 12 inches in width and 1/4 to 1 inch in thickness.

** T-1 steel meets the requirements of ASTM A514 and/or A517 steel.

where subscripts w and f denote the values for web and flange plates, respectively. The critical width-thickness ratio of the web may be of interest in some cases; it is obtained from Eq. 39.

$$\lambda_w = \lambda_f \cdot \left(\frac{b_w}{b_f}\right)\left(\frac{t_f}{t_w}\right) \tag{39}$$

The results are obtained in the same form as the plate buckling curve demonstrated in Fig. 20 for a box-section. The reduction of buckling strength due to the presence of residual stress is similar to that found for the buckling of plates with residual stress. The reduction factors can be obtained similarly as for plates from the curve of critical stress versus width-thickness ratio. Figure 21 shows the reduction factors for a limited number of sections such that the sections containing the assumed residual stresses remain stable until the yield load is reached.

Since the critical width-thickness ratio can be obtained without much difficulty for column cross sections free of residual stress, or found even in the literature[9][10] tabulated for most of the practical column cross sections, the reduction factor makes it possible to determine the critical width-thickness ratio of column cross sections containing residual stress with a simple multiplication.

6. COMPARISON WITH TEST RESULTS

A series of two welded square box-columns of T-1 steel were tested. The section was selected to simulate the plates simply supported at the unloaded edges. The lengths of the test columns were chosen such that column buckling could not occur (upper limit), and at the same time, such that the end disturbances would not affect the plate buckling behavior of the test section as well as the distribution of residual stresses (lower limit). The width-thickness ratios of the specimens were selected such that the critical loads were reached in both the elastic range and in the elastic-plastic range. Two identical specimens were cut from a long fabricated piece for both shapes, thus a total number of four specimens were tested. Table 2 shows the detail of the specimens.

Prior to the buckling tests, tensile coupon tests and residual stress measurements were carried out. The static yield stress had average values of

116 ksi for specimens T-1A and T-1B and

104 ksi for specimens T-2A and T-2B.

Figure 22 shows the distribution of residual stresses in the specimens, from which the following average values of non-dimensionalized compressive residual stresses were obtained.

$$\frac{\sigma_{rc}}{\sigma_Y} = 0.12 \text{ in specimens T-1A and T-1B and}$$

$$\frac{\sigma_{rc}}{\sigma_Y} = 0.16 \text{ in specimens T-2A and T-2B.}$$

Local buckling tests were made under the "as-placed" condition in an 800 kips mechanical type testing machine. The deflection was measured at the center of the width of each side plate at short intervals along the length. The detail of the experiments have been described in Ref.46.

The critical stresses were determined by the so called "top of the knee method"[47] from the load-deflection relationship of the test specimens. Test results are summarized in Table 3 and compared with theoretical predictions in Fig. 23.

The specimens T-1A and T-1B, which buckled in the elastic region, showed good agreement with the prediction, (with a slightly lower stress). Two theoretical predictions were made for specimens T-2A and T-2B, which buckled in the elastic-plastic range; one based on the total strain theory of plasticity and the other based on the incremental theory. The incremental theory predicted no buckling until the specimen reached the yield load, whereas the total strain theory predicted 92% of the yield load. Although both predictions were for loads higher than the test results, the difference is very small for the prediction of the total strain theory. It can be concluded, therefore, that the experiments correlated with the theoretical prediction of elastic and elastic-plastic buckling of steel plates with residual stresses, except for the prediction based on the incremental theory. The lack of correlation of the incremental theory was expected from the results of

experimental studies on aluminum-alloy plates[17][20][23][30].

The test results of both critical stress and ultimate strength are also plotted on the plate buckling curve in Fig. 24, together with the results of similar test on A7 square tubes cited from Ref. 29. The non-dimensionalized comparison of test results in Fig. 24 shows that the welded T-1 plates are stronger than the similar plates of A7 steel. The result was expected from the study on residual stresses and the similar conclusion was obtained in comparison of T-1 and A7 welded columns[48].

The specimens T-1A and T-1B buckled in the elastic range and showed significant post-buckling strength as seen in Fig. 24. On the other hand, T-2A and T-2B buckled in the elastic-plastic range had a relatively small reserve of post-buckling strength.

7. SUMMARY AND CONCLUSIONS

This report has presented the plate buckling strength as well as the local buckling strength of column sections, both containing residual stresses and loaded into the inelastic range of the material. Since the coefficients of the basic differential equation governing plate buckling are variables, it is quite difficult to obtain rigorous solutions. Instead, solutions are obtained on the basis of a finite difference approximation of the differential equation.

The numerical results for plates of various edge conditions are presented in plate buckling curves of non-dimensionalized stress against non-dimensionalized width-thickness ratio, from which reduction factors of width-thickness ratio due to the presence of residual stress are plotted at several stress levels.

The numerical results of local buckling strength were obtained for a few cases.

A series of four welded built-up rectangular tubes of "T-1" constructional alloy steel have been tested to substantiate the theoretical results.

The following conclusions may be drawn from this study for both plate buckling and the local buckling of columns:

(1) The finite difference approximation of the differential equation was found to be quite powerful in obtaining the eigenvalue of the basic differential equation

governing plate buckling.

(2) The elastic buckling strength depends largely on the magnitude and distribution of residual stresses.

(3) The effect of residual stresses on the elastic-plastic buckling depends greatly on the width-thickness ratio of the plates.

(4) A critical value of width-thickness ratio exists; plates with width-thickness ratio less than this critical value sustain the full yielding load.

(5) The incremental theory of plasticity predicts a much higher critical width-thickness ratio (and consequently a much higher critical stress) than the total strain theory.

(6) The comparison with the tests shows correlation between the theoretical results and the test results; for elastic-plastic buckling, the theoretical results based on the total strain theory gives good correlation with the experimental results, but the results based on the incremental theory predict a much higher critical stress.

(7) Comparison of experiments on welded square tubes shows that the tubes of T-1 steel are stronger for local buckling than those of A7 steel when compared on a non-dimensionalized basis.

(8) The square tubes buckled in the elastic range showed a significant post-buckling strength, while the tubes buckled in the elastic-plastic range had a relatively small reserve of post buckling strength.

8. ACKNOWLEDGEMENTS

This study has been carried out as a part of the research project on "Welded Built-Up and Rolled Heat Treated T-1 Steel Columns" being conducted at Fritz Engineering Laboratory, Department of Civil Engineering, Lehigh University.

The project is sponsored by the United States Steel Corporation. Charles G. Shilling of that corporation made many valuable comments, both in the course of the program and in the preparation of this report. Task Group 1 of the Column Research Council of the Engineering Foundation acted in an advisory capacity under the chairmanship of John A. Gilligan.

The authors wish to express their appreciation to the Computer Laboratory, Lehigh University for help in programming, and to Enver Odar for his willing assistance in the performance of the test program.

9. NOMENCLATURE

$\mathbf{A}$	square matrix
$\mathbf{B}$	square matrix
b	width of a plate
C_1, C_2, C_3, C_4	constant coefficients
$C_{1,i}$ to $C_{6,i}, C_i, C'_i$	coefficients to appear in basic difference equation at mesh point i
E	modulus of elasticity, error
E_s	secant modulus of elasticity
E_t	tangent modulus of elasticity
e	$E/E_s - 1$, a subscript to show exact solution
I	moment of inertia
I_o	a constant value of moment of inertia
i	a sequence number used as a subscript
k_1 to k_4	coefficients relating to stress-strain relationship
M	moment
M_y	bending moment per unit length along a line parallel to z-axis
M_z	bending moment per unit length along a line parallel to y-axis
M_{zy}	twisting moment per unit length, $M_{zy} = -M_{yz}$
n	number of mesh cells in width of a plate, number of plate elements to meet at an intersection
p	number of half waves in the z-direction
R	reduction factor of width-thickness ratio

r	width of mesh points
t	thickness of a component plate
w	deflection of a plate
$\mathbb{X}$	eigenvector (column matrix)
Y	a function of Y
x,y,z	cartesian coordinates
γ	shear strain
δ	an operational notation indicating a small value
ϵ_{cr}	strain at buckling load
ϵ_r	residual strain
ϵ_Y	yield strain
ϵ_y	normal strain component parallel to y-axis
ϵ_z	normal strain component parallel to z-axis
λ	non-dimensionalized slenderness ratio, non-dimensionalized width-thickness ratio
μ	ratio of width for unevenly spaced mesh
ν	Poisson's Ratio
σ_{cr}	buckling stress
σ_r	residual stress
σ_{rc}	compressive residual stress at the flange tips
σ_{rt}	tensile residual stress at the center of the flange
σ_Y	static yield stress
σ_z	normal stress component parallel to z-axis
τ	shear stress

10. APPENDICES

APPENDIX A: COEFFICIENTS OF THE BASIC DIFFERENCE EQUATION FOR UNEQUAL SPACING

This appendix compliments the coefficients of basic difference equation, Eq. 15 for an unevenly spaced mesh. The following equations replace the coefficients defined by Eq. 11 for an evenly spaced mesh at mesh point i-1, and i+1 in Fig. 3b.

1. AT MESH POINT j = i+1 IN FIG. 3b

$$C_{1,j} = \frac{I_{j+1}}{I_o} k_{3,j+1}$$

$$C_{2,j} = 2 \frac{I_{j+1}}{I_o} k_{3,j+1} + 2 \frac{I_j}{I_o} k_{3,j} + \frac{\pi^2(\mu r)^2}{L^2} \cdot$$

$$\cdot\left(\frac{I_{j+1}}{I_o} k_{2,j+1} + \frac{I_j}{I_o} k_{2,j} + 4 \frac{I_{j+1/2}}{I_o} k_{4,j+1/2}\right)$$

$$C_{3,j} = \frac{2\mu}{1+\mu} \frac{I_{j+1}}{I_o} k_{3,j+1} + 4 \frac{I_j}{I_o} k_{3,j} + \frac{I_{j-1}}{I_o} k_{3,j-1} + \frac{\pi^2(\mu r)^2}{L^2} \cdot$$

$$\cdot\left(4 \frac{I_j}{I_o} k_{2,j} + 4 \frac{I_{j+1/2}}{I_o} k_{4,j+1/2} + 4 \frac{I_{j-1/2}}{I_o} k_{4,j-1/2}\right.$$

$$\left. + \frac{\pi^2(\pi r)^2}{L^2} \frac{I_j}{I_o} k_{1,j}\right.$$

$$C_{4,j} = 2\mu \frac{I_{j-1}}{I_o} k_{3,j-1} + 2 \frac{I_j}{I_o} k_{3,j} + \frac{\pi^2(\pi r)^2}{L^2} \cdot$$

$$\cdot \left(\frac{I_{j-1}}{I_o} k_{2,j-1} + \frac{I_j}{I_o} k_{2,j} + 4 \frac{I_{j-1/2}}{I_o} k_{4,j-1/2} \right)$$

$$C_{5,j} = \frac{2\mu^2}{1+\mu} \frac{I_{j-1}}{I_o} k_{3,j-1}$$

$$C_j = \frac{12\pi^2}{n^4} \left(\frac{b}{L}\right)^2 \cdot \left(\frac{\sigma_{z,j}}{\sigma_Y}\right) \qquad \text{(A.1)}$$

2. AT MESH POINT i IN FIG. 3b

$$C_{1,i} = \frac{1}{\mu^2} \frac{I_{i+1}}{I_o} k_{3,i+1}$$

$$C_{2,i} = \frac{1}{\mu(1+\mu)} \left[\frac{2(1+\mu)}{\mu} \frac{I_{i+1}}{I_o} k_{3,i+1} + 4 \frac{I_i}{I_o} k_{3,i} \right.$$

$$\left. + \frac{\pi^2 r^2}{L^2} \left(\frac{I_{i+1}}{I_o} k_{2,i+1} + \frac{I_i}{I_o} k_{2,i} + 4 \frac{I_{i+1/2}}{I_o} k_{4,i+1/2} \right) \right]$$

$$C_{3,i} = \frac{1}{\mu^2} \frac{I_{i+1}}{I_o} k_{3,i+1} + \frac{4}{\mu} \frac{I_i}{I_o} k_{3,i} + \frac{I_{i-1}}{I_o} k_{3,i-1} + \frac{\pi^2 r^2}{L^2} \cdot$$

$$\cdot \left(\frac{4}{\mu} \frac{I_i}{I_o} k_{2,i} + \frac{4}{\mu} \frac{I_{i+1/2}}{I_o} k_{4,i+1/2} + 4 \frac{I_{i-1/2}}{I_o} k_{4,i-1/2} \right.$$

$$\left. + \frac{\pi^2 r^2}{L^2} \frac{I_i}{I_o} k_{1,i} \right)$$

$$C_{4,i} = \frac{1}{1+\mu} \left[2(1+\mu) \frac{I_{j-1}}{I_o} k_{3,i-1} + 4 \frac{I_i}{I_o} k_{3,i} \right.$$

$$+ \frac{\pi^2 r^2}{L^2}\left(2\,\frac{I_{i-1}}{I_o}\,k_{2,i-1} + 2\,\frac{I_i}{I_o}\,k_{2,i} + 4\,\frac{I_{i-\frac{1}{2}}}{I_o}\,k_{4,i-\frac{1}{2}}\right)\Bigg]$$

$$C_{5,i} = \frac{I_{i-1}}{I_o}\,k_{3,i-1}$$

$$C_i = \frac{12\pi^2}{n^4}\left(\frac{b}{L}\right)^2\left(\frac{\sigma_{z,i}}{\sigma_Y}\right) \qquad \text{(A.2)}$$

3. AT MESH POINT j = i-1 IN FIG. 3b

$$C_{1,j} = \frac{1}{\mu(1+\mu)}\,\frac{I_{j+1}}{I_o}\,k_{3,j+1}$$

$$C_{2,j} = \frac{2}{\mu}\,\frac{I_{j+1}}{I_o}\,k_{3,j+1} + 2\,\frac{I_j}{I_o}\,k_{3,j} + \frac{\pi^2 r^2}{L^2}\cdot$$

$$\cdot\left(\frac{I_{j+1}}{I_o}\,k_{2,j+1} + \frac{I_j}{I_o}\,k_{2,i} + 4\,\frac{I_{j+\frac{1}{2}}}{I_o}\,k_{4,j+\frac{1}{2}}\right)$$

$$C_{3,j} = \frac{2}{1+\mu}\,\frac{I_{j+1}}{I_o}\,k_{3,j+1} + 4\,\frac{I_j}{I_o}\,k_{3,j} + \frac{I_{j-1}}{I_o}\,k_{3,j-1}$$

$$+ \frac{\pi^2 r^2}{L^2}\left(4\,\frac{I_j}{I_o}\,k_{2,j} + 4\,\frac{I_{j+\frac{1}{2}}}{I_o}\,k_{4,j+\frac{1}{2}} + 4\,\frac{I_{j-\frac{1}{2}}}{I_o}\,k_{4,j-\frac{1}{2}}\right.$$

$$\left. + \frac{\pi^2 r^2}{L^2}\,\frac{I_j}{I_o}\,k_{1,j}\right)$$

$$C_{4,j} = 2\,\frac{I_{j-1}}{I_o}\,k_{3,j-1} + 2\,\frac{I_j}{I_o}\,k_{3,j} + \frac{\pi^2 r^2}{L^2}\cdot$$

$$\cdot\left(\frac{I_{j-1}}{I_o}\,k_{2,j-1} + \frac{I_j}{I_o}\,k_{2,j} + 4\,\frac{I_{j-\frac{1}{2}}}{I_o}\,k_{4,j-\frac{1}{2}}\right)$$

$$C_{5,j} = \frac{I_{j-1}}{I_o} k_{3,j-1}$$

$$C_j = \frac{12\pi^2}{n^4} \left(\frac{b}{L}\right)^2 \left(\frac{\sigma_{z,j}}{\sigma_Y}\right) \qquad \text{(A.3)}$$

APPENDIX B: DETERMINATION OF COEFFICIENTS OF THE DIFFERENCE EQUATION

Appendix B substantiates the equations in computing the coefficients of finite difference equations as described in Art. 4.1.

The strain distribution due to external thrust under which the plate will buckle is specified. The external thrust and the width-thickness ratio of the plate are computed under this external strain distribution. The residual strains as well as the external strains are given at the edges of mesh cells and at the edges of the plate elements and they are assumed to change linearly inside a mesh cell. As seen in Figs. 25a and 25b, the number of necessary data for a plate with n mesh points is n+1, when the plate ends on half-integer stations. Similarly, for a cross section as seen in Fig. 25c, n+3 data are necessary for n mesh points.

Consider the i-th cell and compute the moduli and the thrust acting on the mesh cell. The strains at both edges of the cell are

$$\epsilon_{i-1} = \epsilon_{r,i-1} + \epsilon_{cr,i-1} \qquad \epsilon_i = \epsilon_{r,i} + \epsilon_{cr,i} \qquad \text{(B.1)}$$

where ϵ_{cr} and ϵ_r denote strain due to external load and residual strain, respectively, and the subscripts i-1 and i

show the strains at the edges of i-th segments as shown in Fig. 25. When the strains exceed the yield strain, a function of strain, e, is defined at both edges (by the total strain theory) by

$$e_{i-1} = \frac{\epsilon_{i-1}}{\epsilon_Y} - 1 \qquad e_i = \frac{\epsilon_i}{\epsilon_Y} - 1 \qquad \text{(B.2)}$$

where ϵ_Y is the yield strain. The average thrust at the i-th mesh cell as well as the coefficients k_1 through k_4 are obtained by the following equations depending on the strains at the edges

(1) $\epsilon_i \geq \epsilon_Y, \qquad \epsilon_{i-1} \geq \epsilon_Y$

$$\left(\frac{\sigma_z}{\sigma_Y}\right)_i = 1$$

$$k_{1,i} = \frac{\dfrac{1}{5-4\nu+3e_i} - \dfrac{1}{5-4\nu+3e_{i-1}}}{\ln\left(\dfrac{5-4\nu+3e_{i-1}}{5-4\nu+3e_i}\right)} \qquad \text{(B.3)}$$

$$k_{2,i} = 2k_1$$

$$k_{3,i} = 4k_1$$

$$k_{4,i} = \frac{\dfrac{1}{2+2\nu+3e_i} - \dfrac{1}{2+2\nu+3e_{i-1}}}{\ln\left(\dfrac{2+2\nu+3e_{i-1}}{2+2\nu+3e_i}\right)}$$

(2) $\epsilon_i \geq \epsilon_Y, \qquad \epsilon_{i-1} < \epsilon_Y$

$$\left(\frac{\sigma_z}{\sigma_Y}\right)_i = 1 - 0.5\,\frac{(1-\epsilon_{i-1})^2}{\epsilon_i - \epsilon_{i-1}}$$

$$k_{1,i} = \frac{1}{\dfrac{\ln\left(\dfrac{5-4\nu}{5-4\nu+3e_i}\right)}{\dfrac{1}{5-4\nu+3e_i} - \dfrac{1}{5-4\nu}} \cdot \dfrac{\epsilon_{i-1}}{\epsilon_i - \epsilon_{i-1}} + (1-\nu^2)\dfrac{1-\epsilon_{i-1}}{\epsilon_i - \epsilon_{i-1}}}$$

$$k_{2,i} = \frac{1}{\dfrac{\ln\left(\dfrac{5-4\nu}{5-4\nu+3e_i}\right)}{\dfrac{1}{5-4\nu+3e_i} - \dfrac{1}{5-4\nu}} \cdot \dfrac{\epsilon_{i-1}}{2(\epsilon_i - \epsilon_{i-1})} + (1-\nu^2)\dfrac{1-\epsilon_{i-1}}{\epsilon_i - \epsilon_{i-1}}}$$

$$k_{3,i} = \frac{4}{\dfrac{\ln\left(\dfrac{5-4\nu}{5-4\nu+3e_i}\right)}{\dfrac{1}{5-4\nu+3e_i} - \dfrac{1}{5-4\nu}} \cdot \dfrac{\epsilon_{i-1}}{\epsilon_i - \epsilon_{i-1}} + 4(1-\nu^2) \cdot \dfrac{1-\epsilon_{i-1}}{\epsilon_i - \epsilon_{i-1}}} \qquad \text{(B.4)}$$

$$k_{4,i} = \frac{1}{\dfrac{\ln\left(\dfrac{2+2\nu}{2+2\nu+3e_i}\right)}{\dfrac{1}{2+2\nu+3e_i} - \dfrac{1}{2+2\nu}} \cdot \dfrac{\epsilon_{i-1}}{\epsilon_i - \epsilon_{i-1}} + (2+2\nu) \cdot \dfrac{1-\epsilon_{i-1}}{\epsilon_i - \epsilon_{i-1}}}$$

(3) $\epsilon_i < \epsilon_Y \qquad \epsilon_{i-1} \geq \epsilon_Y$

The equations are the same as Eq. B.4 if ϵ_i and e_i are interchanged with ϵ_{i-1} and e_{i-1}, respectively.

(4) $\epsilon_i < \epsilon_Y \qquad \epsilon_{i-1} < \epsilon_Y$

$$\left(\frac{\sigma_z}{\sigma_{Yi}}\right) = \frac{\epsilon_i + \epsilon_{i-1}}{2\epsilon_Y}$$

$$k_{1,i} = \frac{1}{1-\nu^2}$$

$$k_{2,i} = \frac{\nu}{1-\nu^2} \qquad \text{(B.5)}$$

$$k_{3,i} = \frac{1}{1-\nu^2}$$

$$k_{4,i} = \frac{1}{2(1+\nu)}$$

The averaging at cells 0 and n in Figs. 25b and 25c must be made with the values at the edges of the plate and those at the edge of the cells. Similarly, the averaging at the intersection j in Fig. 25c must be made with quantities at three points j-1, $\overline{j}$ and j.

Since the plate thickness is assumed constant for each plate element, the averaging of the moment of inertia of the plate is necessary only for local buckling of column

cross sections at the intersection of plate elements. Usually, there is no relation between depth of the web and width of a flange and, consequently, it is convenient to change the width of the mesh at the intersection for each plate element. The average value of moment of inertia is represented as follows at the intersection as shown in Fig. 25c which appears in cross sections such as rectangular box, channel and angle

$$I_i = (1 + \mu) \frac{I_1 I_2}{\mu I_1 + I_2} \tag{B.6}$$

When two identical plates and another plate meet at an intersection, which is the case for cross sections such as H and tee , the two identical plates can be considered as if they are a plate with moment of inertia of $2I_1$; thus the average inertia at the point is

$$I_i = (1 + \mu) \frac{2I_1 I_2}{2\mu I_1 + I_2} \tag{B.7}$$

Substituting the above quantities into Eq. 11, or into the equations in Appendix A depending on the problem, simultaneous finite difference equations are obtained, from which the critical width-thickness ratios can be determined together with suitable boundary conditions.

The critical stress corresponding to the specified strain is computed simply as the sum of average thrust at each mesh cell. For a plate which ends on half-integer

stations, the critical thrust is, in the non-dimensionalized form

$$\frac{\bar{\sigma}_{cr}}{\bar{\sigma}_Y} = \sum_{i=1}^{n} \left(\frac{\bar{\sigma}_Z}{\bar{\sigma}_Y}\right)_i \qquad (B.8)$$

and for a plate ending on integer stations, it is

$$\frac{\bar{\sigma}_{cr}}{\bar{\sigma}_Y} = \sum_{i=1}^{n} \left(\frac{\bar{\sigma}_Z}{\bar{\sigma}_Y}\right) - \frac{1}{2}\left[\left(\frac{\bar{\sigma}_Z}{\bar{\sigma}_Y}\right)_o \quad \left(\frac{\bar{\sigma}_Z}{\bar{\sigma}_Y}\right)_n\right] \qquad (B.9)$$

The critical stress for a cross section is obtained by considering the same equations as above for each plate element.

APPENDIX C: COMPARISON OF DIRECT METHOD AND ITERATIVE METHOD IN DETERMINING EIGENVALUE OF A MATRIX

The generally accepted criterion of the advantage of a given computational scheme is the number of necessary multiplications and divisions and also additions and subtractions. Fundamental to this, is the number of multiplications and divisions and, therefore, methods are compared from this point of view. Simplicity and uniformity of the operations to be performed, as well as the coding program, may be one of the factors to be considered. Another important factor influencing the choice of a computational scheme is the absence of a loss of significant figures in the process of computation.

From the viewpoint of simplicity and uniformity, the iterative method is preferable. The matrix inversion and multiplication routines may be available as common computer library routines. The scheme for iteration itself is also simple. Once the coding is made, the program automatically converges to the desired eigenvalue and thus no "guess work" is necessary. It is noted in the literature[41][42][43] that the iterative method is the easiest and the most preferable when only the largest or the smallest eigenvalue is sought and the existence of such a real eigenvalue is guaranteed. In a case of a physical problem such as the

buckling of a plate, the above conditions are satisfied and the method may be preferable. The number of operations necessary to invert an n by n matrix is approximately n^3 by the Gaussian elimination method, and the number for one iteration to obtain the eigenvalue is roughly n^2.

It is important to note that the best method also depends on the problem at hand and will not always be any one particular method. The discussion on a particular matrix equation is limited to the finite difference solution of Eq. 9. Sparseness is the characteristic of the matrices of this buckling problem. The reduction of the number of operations due to the sparseness is less than half for inverting the matrix A in Eq. 28 as long as the elimination scheme is used. The resulting A^{-1} is no longer a sparse matrix and, therefore, the sparseness of the original matrix does not contribute to cutting the operation for the iteration to the eigenvalue. The sparseness of the matrices, as discussed, does not reduce the total operation dramatically in any sense.

The method to find the eigenvalue directly from Eq.29 is not recommended, generally, except for the case of such a small matrix where the number of operations in obtaining solutions has no importance. The method considered now is a trial and error method designed to find the eigenvalue by evaluating the determinant of Eq. 29. Fortunately, it is not difficult to estimate the bounds within which the

solution of the present problem exists. Since analytical solutions can be obtained easily for plates without residual stress, such solutions will furnish the basis for estimating the bounds of solution when plates with residual stress are solved by the finite difference method. Similarly, analytical solutions for each component plate of column cross sections give some idea for estimating the local buckling solutions of the sections. Once the bound is obtained, a limited number of trials may result in a solution with the desired accuracy.

The major computation of this trial method is to evaluate the determinant

$$\Delta = \left| /\!A - \lambda^2 /\!B \right| \tag{29}$$

The trial value of eigenvalue affects only the diagonal matrix $/\!B$; thus, the number of operations needed to set up the terms of the matrix, of which the determinant is evaluated, is equal to n per each trial after the initial setup of $/\!A$ and $/\!B$ matrices are made. The determinant can be evaluated by the elimination scheme, since the terms on the main diagonal are dominant in any case of matrices which are generated for the finite difference solution of the differential equation. The number of operations are reduced significantly because of the sparesness. Only five multiplication processes and ten division processes are necessary for each row of the matrix, thus, the total number of multiplication and division processes necessary

to evaluate an n by n matrix is roughly 15 n. It is quite important that the order of the necessary computation is not squared or cubed, but of the first power matrix size.

Supposing fifteen iterations are necessary to converge for a certain desired accuracy by the iterative method, the total operations are roughly $n^3 + 15n^2$, whereas if 20 trials result in the same accuracy with the trial and error method, the number of total operations necessary is 300n. The above number of iterations and trials are good averages obtained by actual computations. Equating these numbers, it may be concluded that the iterative procedure is preferable, roughly, for a 10 by 10 or smaller matrix and the trial method is suitable, roughly, for a 15 by 15 or larger matrix. Coding of the matrix operation for the trial method is far easier than the iterative method, however, an additional effort is necessary in order to "guess" the bounds in which the solution is present.

Although the trial method may converge to the eigenvalue second in line instead of the smallest, such an error is easily detected by checking the eigenvector corresponding to the eigenvalue as to whether the buckled shape is compatible with the expected buckling mode.

Concluding the comparison, the direct method with trial and error is definitely preferable for a larger matrix, while for a smaller size matrix both methods are

equally good; the trial method is easy to code but needs additional "guess work", and the iterative method needs more coding efforts but results in a straight forward operation for determining the solution.

11. TABLES AND FIGURES

TABLE 1 ASSUMPTIONS OF INELASTIC PLATE BUCKLING THEORY

Investigator*	Stress-Strain Law	Poisson's Ratio	Plasticity Law	Buckling Model
Bijlaard[15]	Incremental and Deformation	Instantaneous	Octahedral Shear	No Strain Reversal
Handelman[21] Prager	Incremental	Instantaneous	Octahedral Shear	Strain Reversal
Pearson[22]	Incremental	Instantaneous	Octahedral Shear	No Strain Reversal
Ilyushin[19]	Deformation	0.5	Octahedral Shear	Strain Reversal
Stowell[20]	Deformation	0.5	Octahedral Shear	No Strain Reversal

*The numbers in parenthesis refers to the list of references.

TABLE 2 DETAIL OF SPECIMENS

ece o.	Length in.	Description	Basic Tests	Specimen No.	Length in.	L/b	b/t*
1	200	11-1/2 x 11-1/2 x 1/4 in. Box	Coupons	T-1A	60	5.31	44.0
			Residual stress	T-1B	60	5.34	44.0
2	140	7 x 7 x 1/4 in. Box	Coupons	T-2A	35	5.18	26.2
			Residual Stress	T-2B	35	5.18	26.2

*Average of four plates

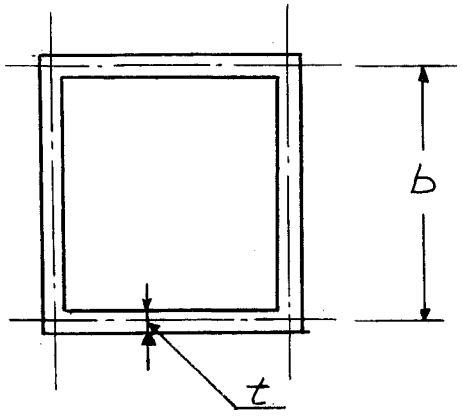

TABLE 3 SUMMARY OF PLATE BUCKLING TESTS

pecimen	$\frac{b}{t}\Big/\sqrt{\frac{\sigma_y}{E}}$	σ_{rc}/σ_Y	P_{max} Kips	P_{cr} Kips	P_{max}/P_Y Test	P_{cr}/P_Y Test	P_{cr}/P_Y Predicted
T-1A	2.61	0.12	700	520	0.53	0.39	0.43
T-1B	2.61	0.12	694	510	0.52	0.38	0.43
T-2A	1.64	0.16	651	630	0.90	0.87	0.91
T-2B	1.64	0.16	657	645	0.91	0.89	0.91

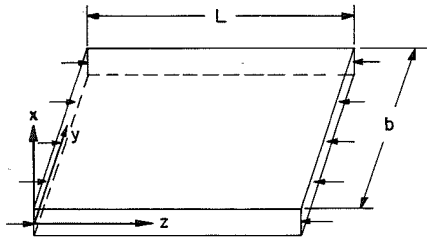

(a) Coordinate Axes for Plates

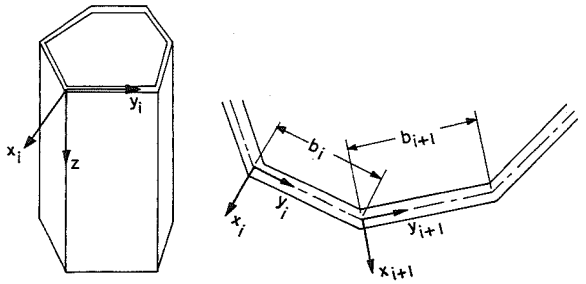

(b) Coordinate Axes for Plate Assemblies

FIG. 1 COORDINATE AXES FOR ANALYSIS OF LOCAL BUCKLING

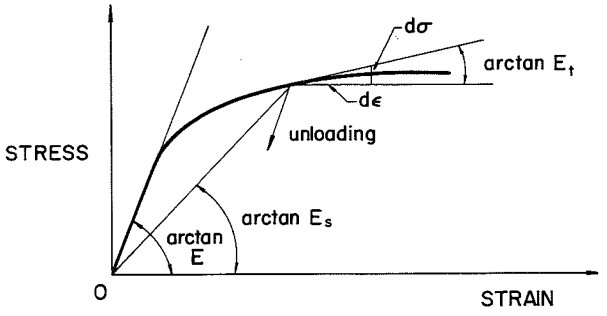

(a) GENERAL CASE

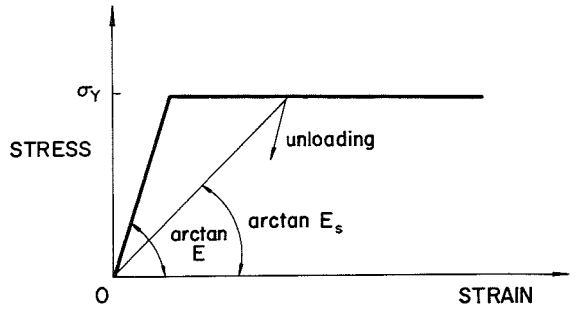

(b) IDEALIZED RELATIONSHIP FOR STEEL (ELASTIC PERFECTLY PLASTIC MATERIAL)

FIG. 2 STRESS-STRAIN RELATIONSHIP

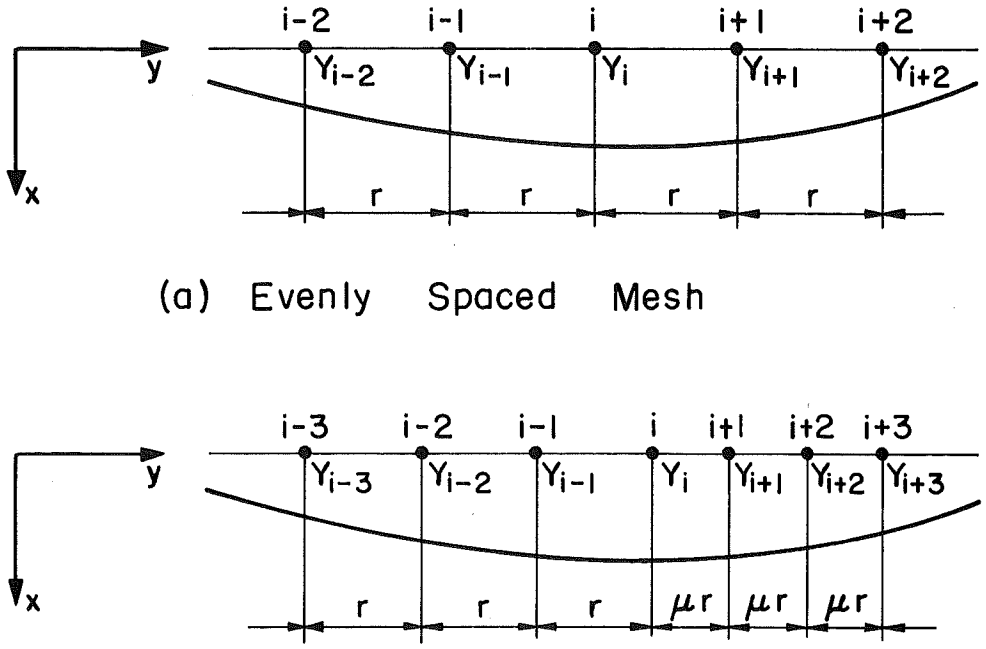

FIG. 3 MESH FOR FINITE DIFFERENCES

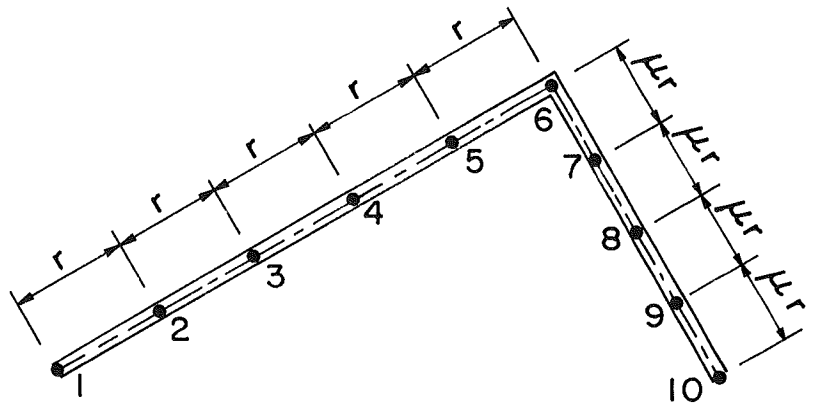

FIG. 4 EXAMPLE OF MESH ON ANGLE SECTION

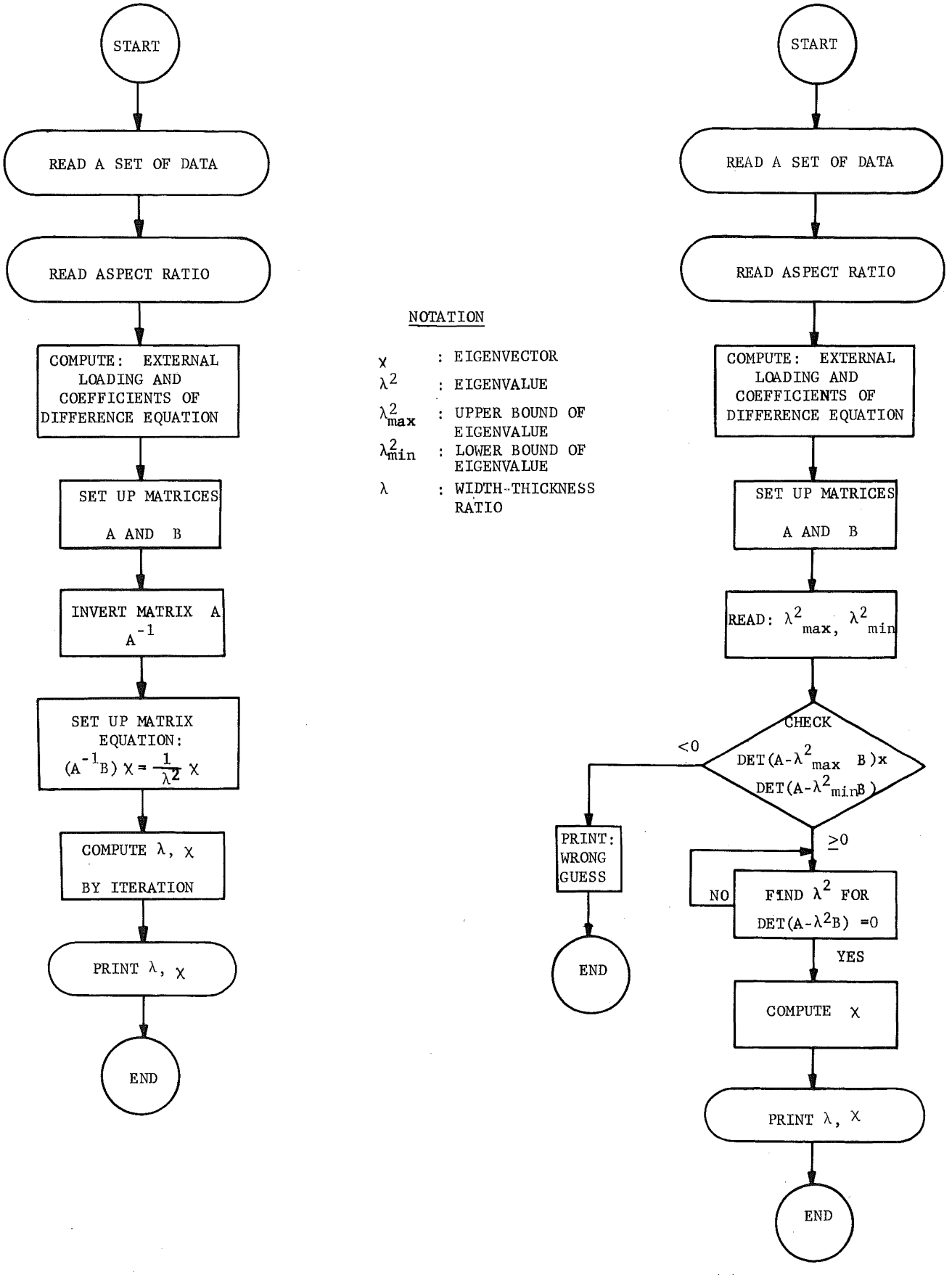

(a) ITERATIVE METHOD

(b) DIRECT METHOD

FIG. 5 SCHEMATIC DIAGRAM FOR CRITICAL WIDTH-THICKNESS RATIO AND ASPECT RATIO RELATIONSHIP

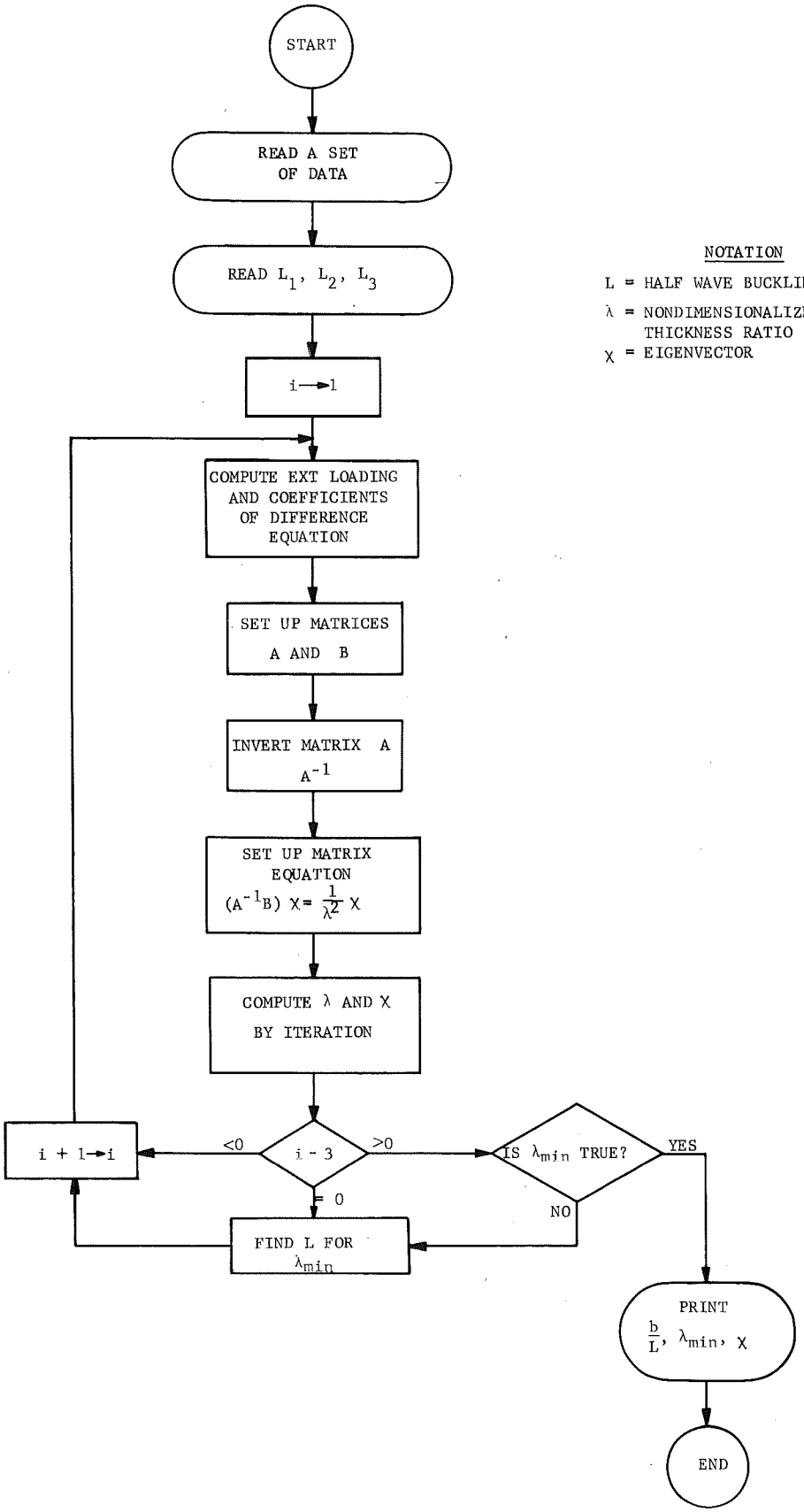

NOTATION

L = HALF WAVE BUCKLING LENGTH

λ = NONDIMENSIONALIZED WIDTH-THICKNESS RATIO

X = EIGENVECTOR

(a) Cooling Pattern 1

$|\sigma_{rt}| = |\sigma_{rc}|$

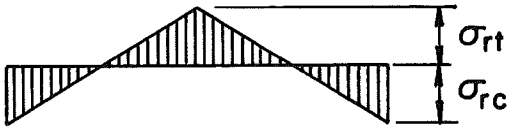

(b) Cooling Pattern 2

$|\sigma_{rt}| = |\sigma_{rc}|$

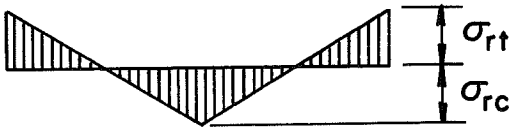

(c) Welding Pattern 1

$\sigma_{rt} = \sigma_Y$

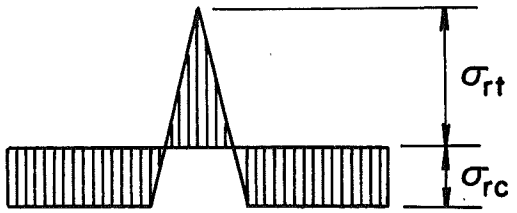

(d) Welding Pattern 2

$\sigma_{rt} = \sigma_Y$

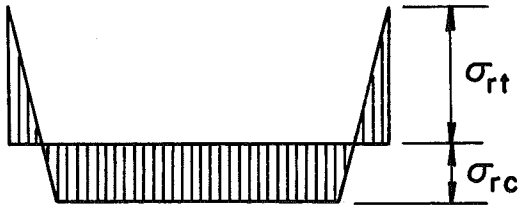

FIG. 7 IDEALIZED RESIDUAL STRESS DISTRIBUTION

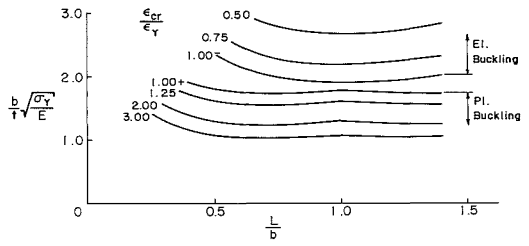

(a) Free of Residual Stress

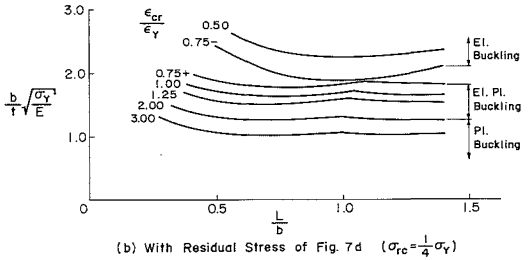

(b) With Residual Stress of Fig. 7d ($\sigma_{rc}=\frac{1}{4}\sigma_Y$)

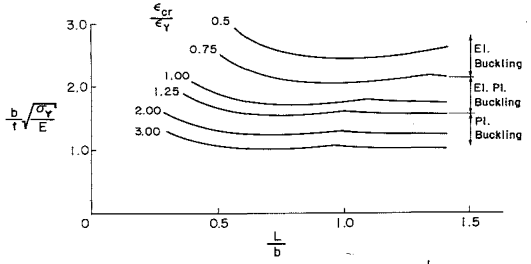

(c) With Residual Stress of Fig. 7b ($\sigma_{rc}=\frac{1}{4}\sigma_Y$)

FIG. 8 WIDTH-THICKNESS RATIO AND ASPECT RATIO RELATIONSHIP (PLATES SIMPLY SUPPORTED AT UNLOADED EDGES)

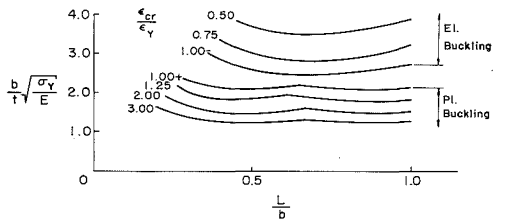

(a) Free of Residual Stress

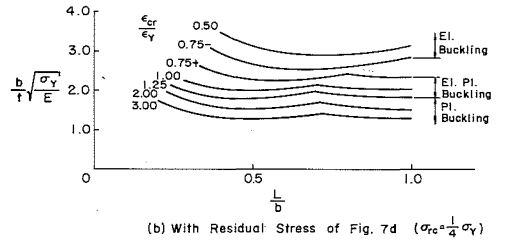

(b) With Residual Stress of Fig. 7d ($\sigma_{rc}=\frac{1}{4}\sigma_Y$)

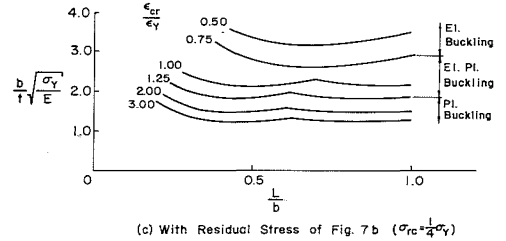

(c) With Residual Stress of Fig. 7b ($\sigma_{rc}=\frac{1}{4}\sigma_Y$)

FIG. 9 WIDTH-THICKNESS RATIO AND ASPECT RATIO RELATIONSHIP (PLATES FIXED AT UNLOADED EDGES)

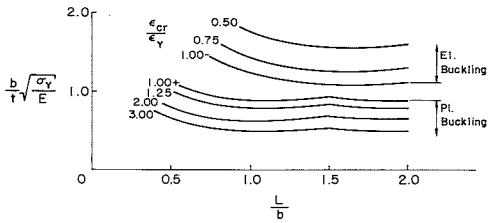

(a) Free of Residual Stress

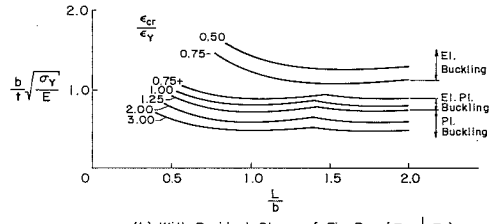

(b) With Residual Stress of Fig. 7c ($\sigma_{rc}=\frac{1}{4}\sigma_Y$)

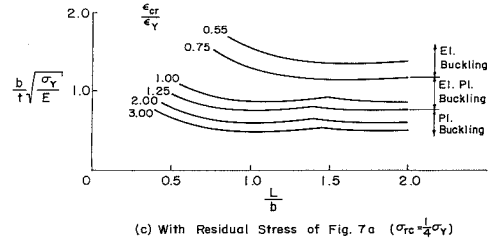

(c) With Residual Stress of Fig. 7a ($\sigma_{rc}=\frac{1}{4}\sigma_Y$)

FIG. 10 WIDTH-THICKNESS RATIO AND ASPECT RATIO RELATIONSHIP (PLATES FIXED AND FREE AT LOADED EDGES)

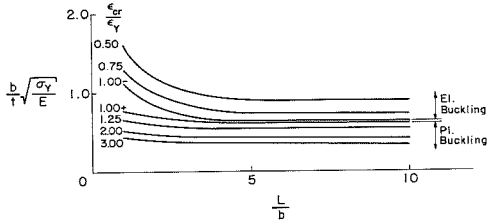

(a) Free of Residual Stress

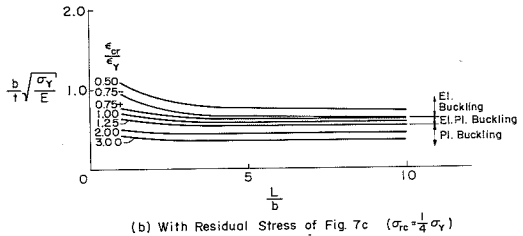

(b) With Residual Stress of Fig. 7c ($\sigma_{rc}=\frac{1}{4}\sigma_Y$)

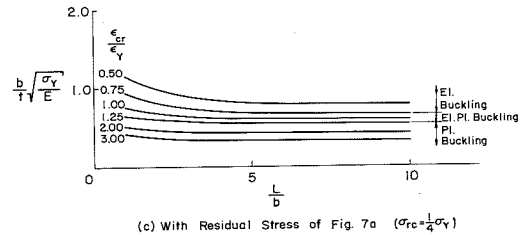

(c) With Residual Stress of Fig. 7a ($\sigma_{rc}=\frac{1}{4}\sigma_Y$)

FIG. 11 WIDTH-THICKNESS RATIO AND ASPECT RATIO RELATIONSHIP (PLATES SIMPLY SUPPORTED AND FREE AT UNLOADED EDGES)

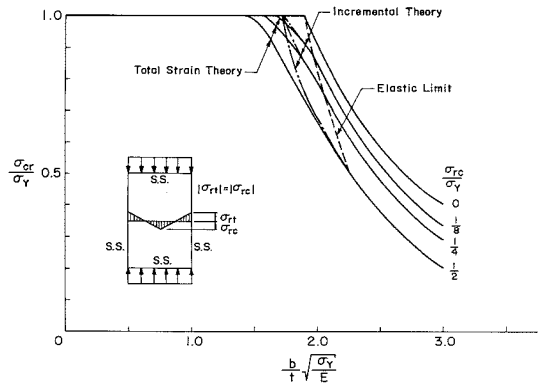

(a) With Residual Stress of Cooling Pattern

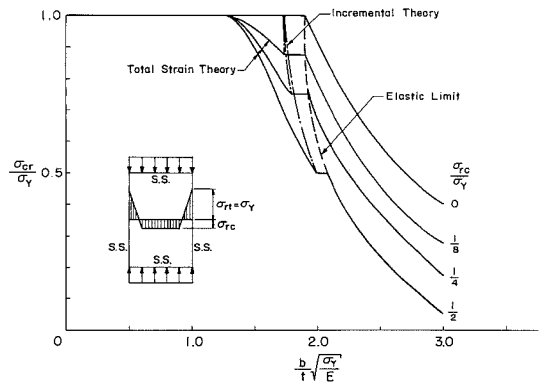

(b) With Residual Stress of Welding Pattern

FIG. 12 PLATE BUCKLING CURVE (PLATE SIMPLY SUPPORTED AT UNLOADED EDGES)

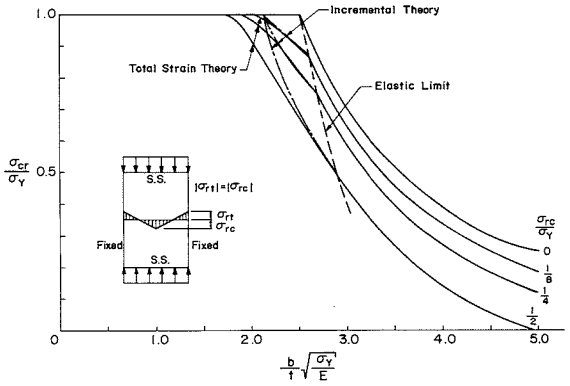

(a) With Residual Stress of Cooling Pattern

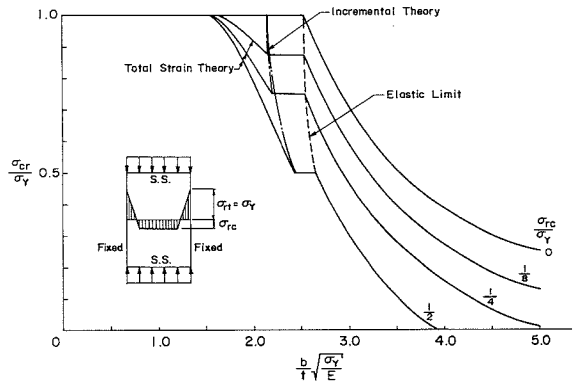

(b) With Residual Stress of Welding Pattern

FIG. 13 PLATE BUCKLING CURVE (PLATE FIXED AT UNLOADED EDGES

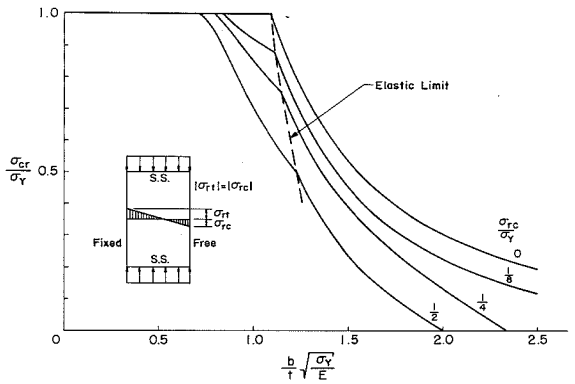

(a) With Residual Stress of Cooling Pattern

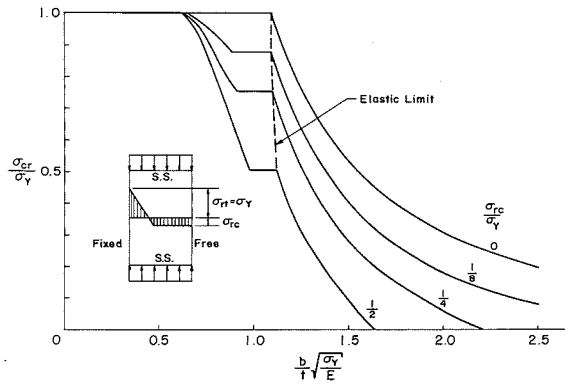

(b) With Residual Stress of Welding Pattern

FIG. 14 PLATE BUCKLING CURVE (PLATE FIXED AND FREE AT UNLOADED EDGES, TOTAL STRAIN THEORY)

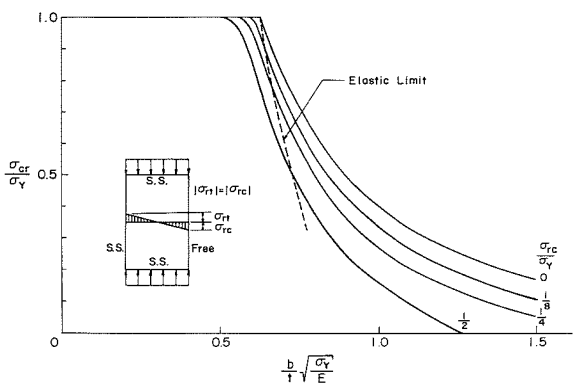

(a) With Residual Stress of Cooling Pattern

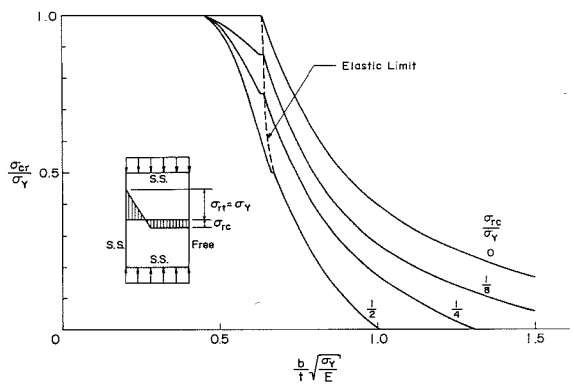

(b) With Residual Stress of Welding Pattern

FIG. 15 PLATE BUCKLING CURVE (PLATE SIMPLY SUPPORTED AND FREE AT UNLOADED EDGES, TOTAL STRAIN THEORY)

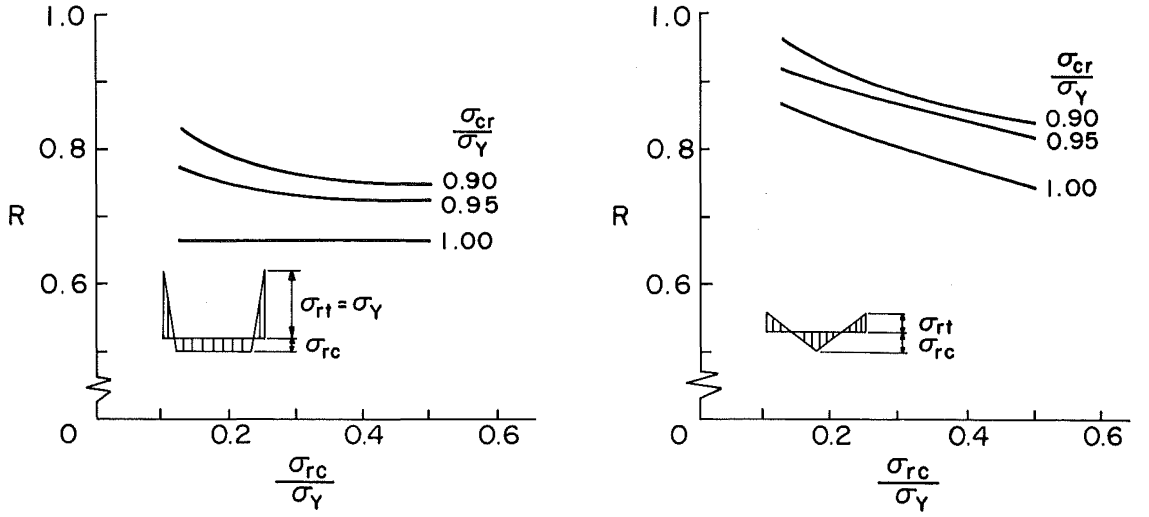

(a) Welding Residual Stress (b) Cooling Residual Stress

FIG. 16 REDUCTION OF CRITICAL WIDTH-THICKNESS RATIO (SIMPLY SUPPORTED PLATES, TOTAL STRAIN THEORY)

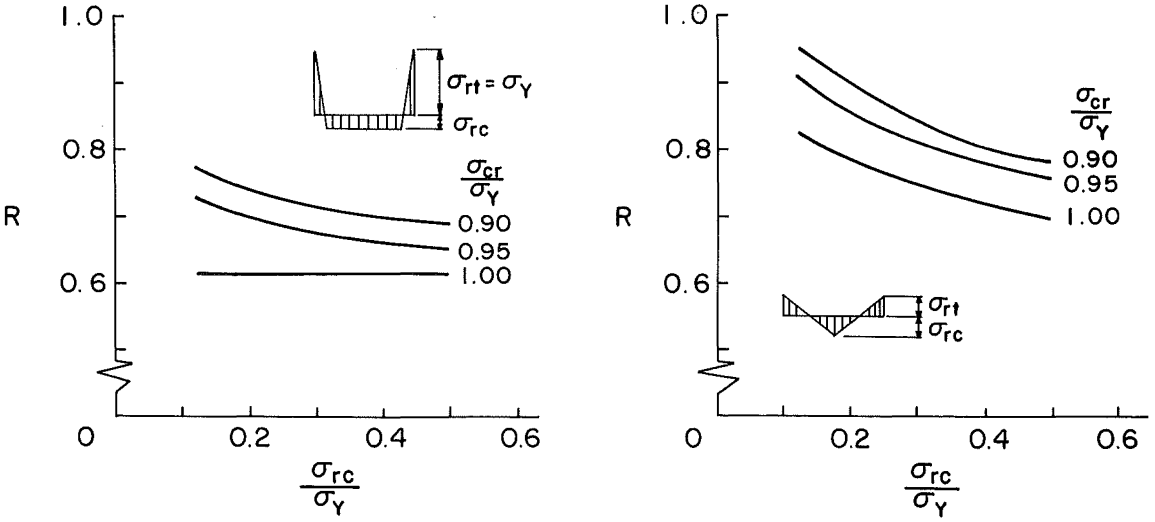

(a) Welding Residual Stress (b) Cooling Residual Stress

FIG. 17 REDUCTION OF CRITICAL WIDTH-THICKNESS RATIO (PLATES FIXED AT UNLOADED EDGES, TOTAL STRAIN THEORY)

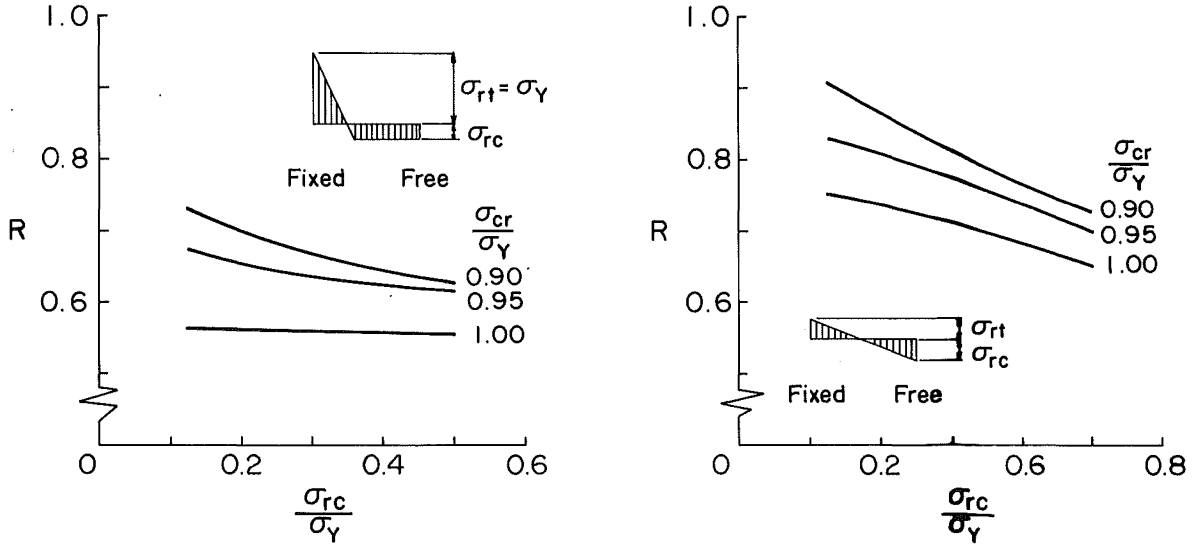

(a) Welding Residual Stress (b) Cooling Residual Stress

FIG. 18 REDUCTION OF CRITICAL WIDTH-THICKNESS RATIO (PLATES FIXED AND FREE AT UNLOADED EDGES, TOTAL STRAIN THEORY)

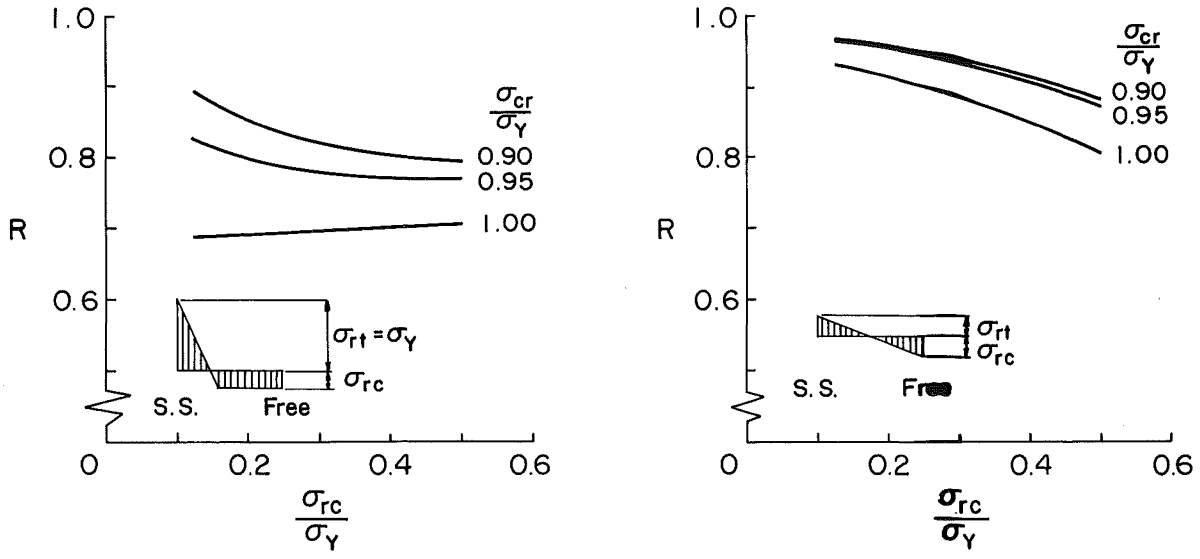

(a) Welding Residual Stress (b) Cooling Residual Stress

FIG. 19 REDUCTION OF CRITICAL WIDTH-THICKNESS RATIO (PLATES SIMPLY SUPPORTED AND FREE AT UNLOADED EDGES, TOTAL STRAIN THEORY)

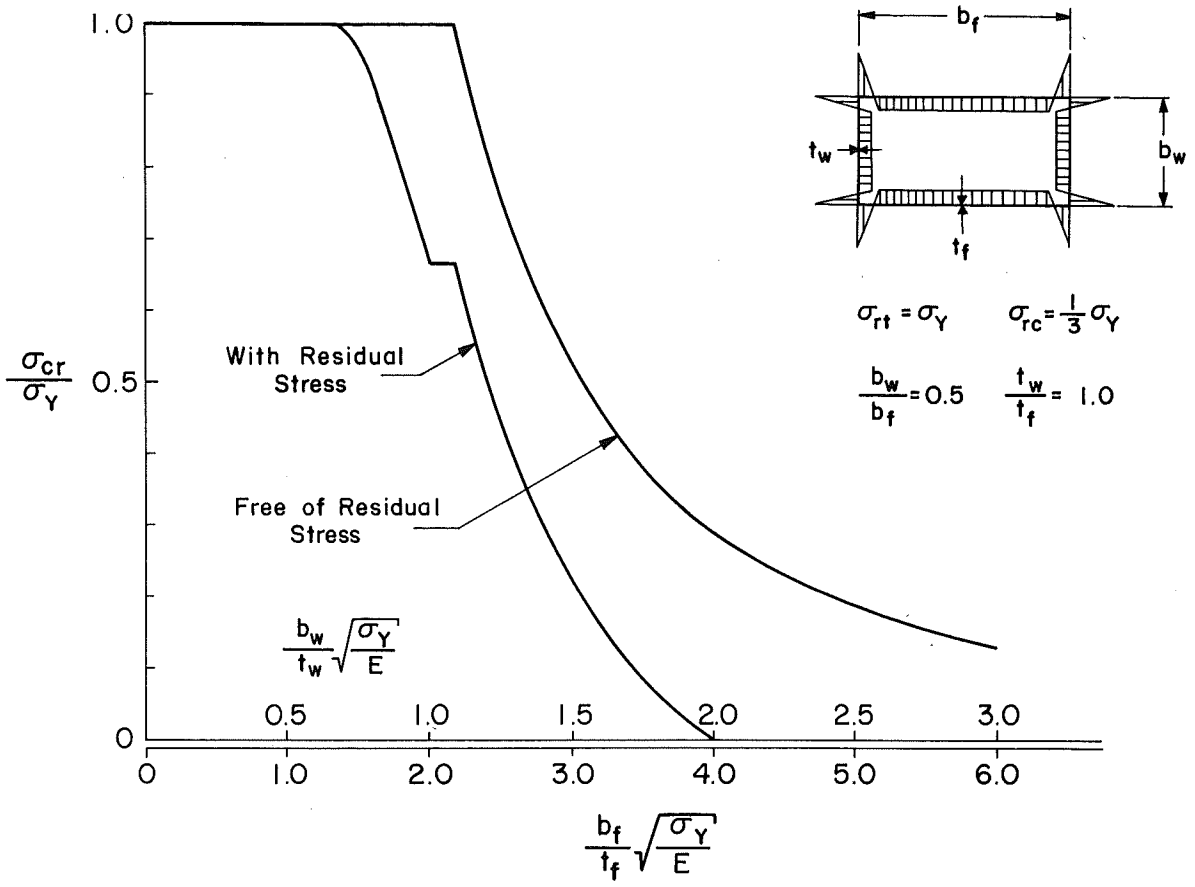

FIG. 20 LOCAL BUCKLING CURVE

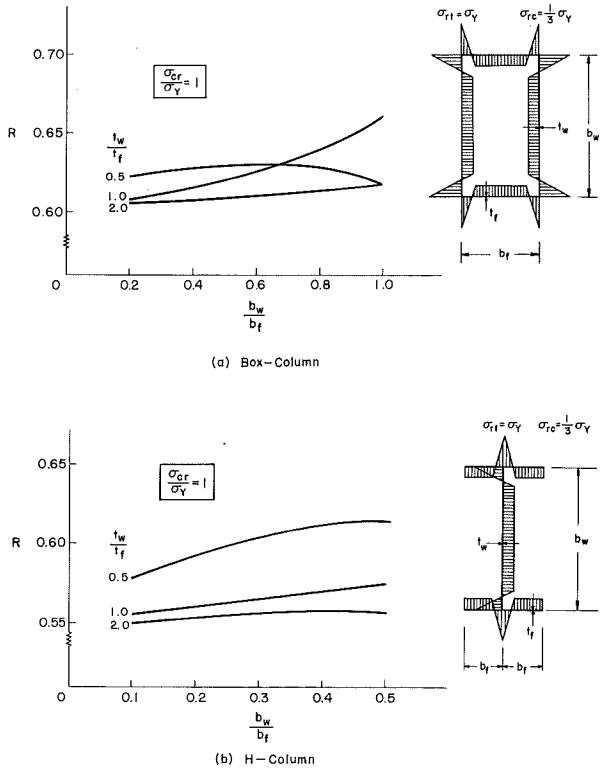

FIG. 21 REDUCTION FACTOR OF WIDTH-THICKNESS RATIO

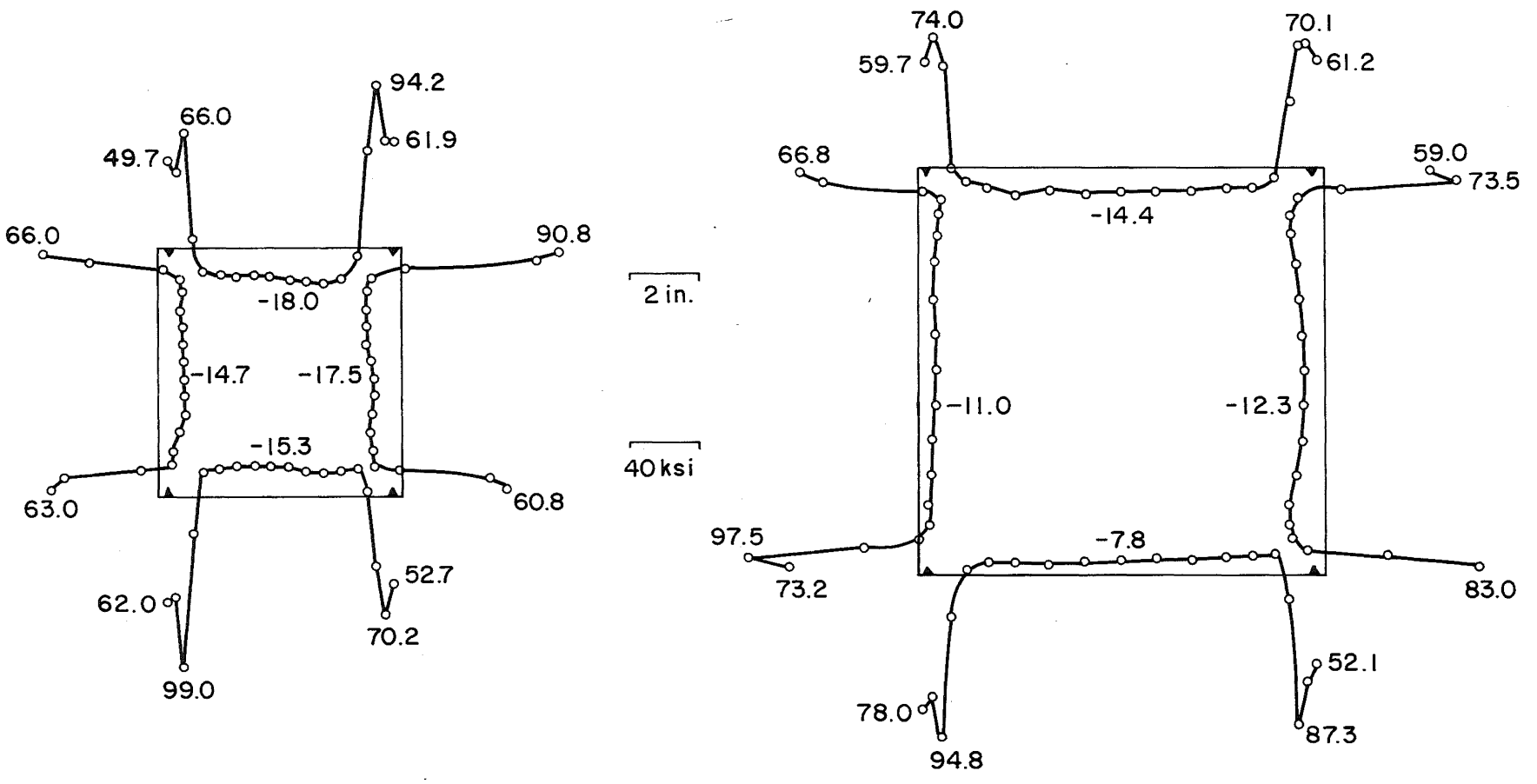

Piece 1 (T-1A,T-1B)

Piece 2 (T-2A,T-2B)

FIG. 22 RESIDUAL STRESS DISTRIBUTIONS IN TEST SPECIMENS

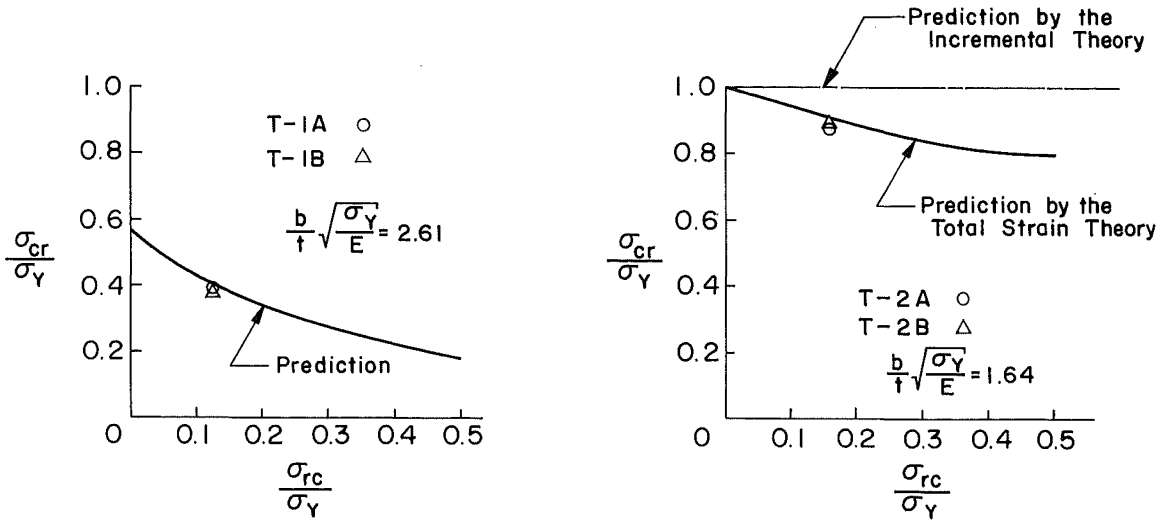

(a) Tests T-1A and T-1B (b) Tests T-2A and T-2B

FIG. 23 COMPARISON WITH LOCAL BUCKLING TEST AND PREDICTION

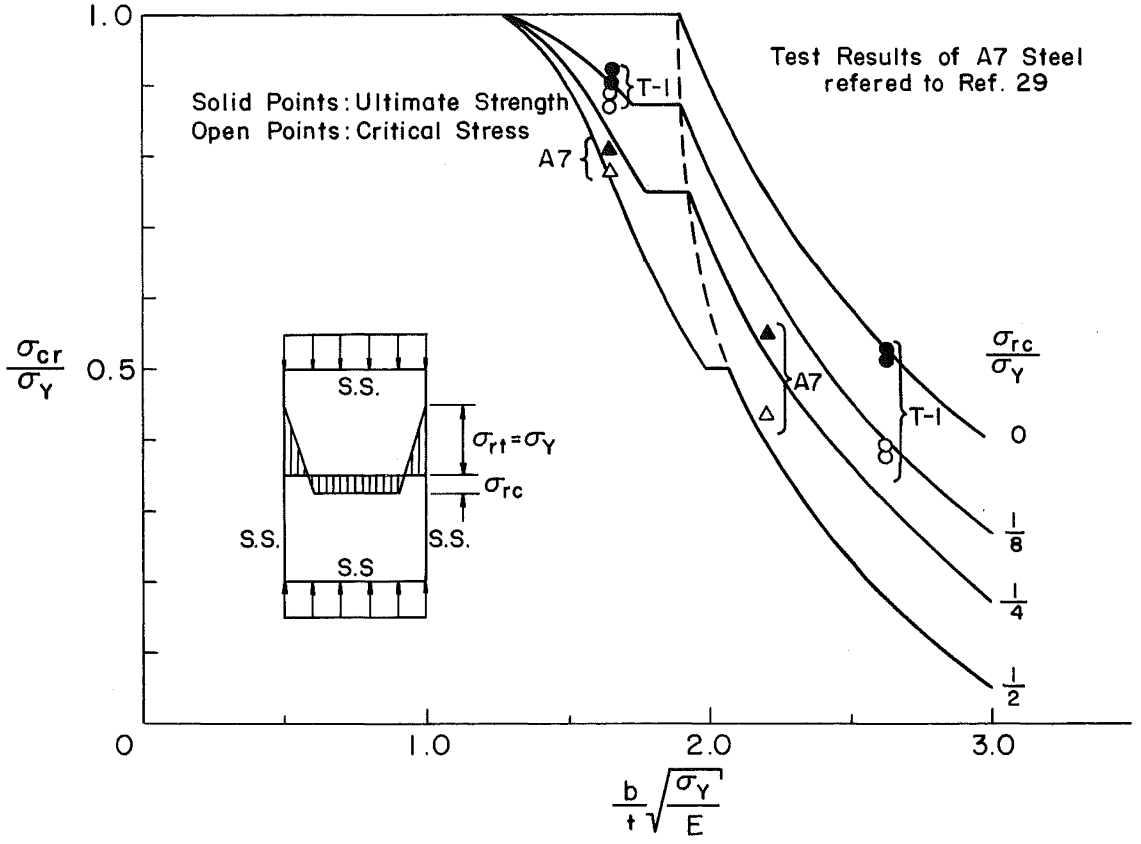

FIG. 24 LOCAL BUCKLING TESTS OF WELDED SQUARE TUBES OF A7 AND T-1 STEELS

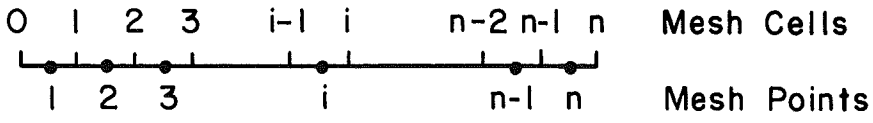

(a) Plate Ends on Half-Integer Stations

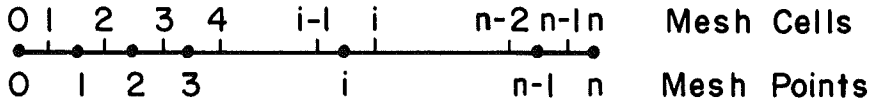

(b) Plate Ends on Integer Stations

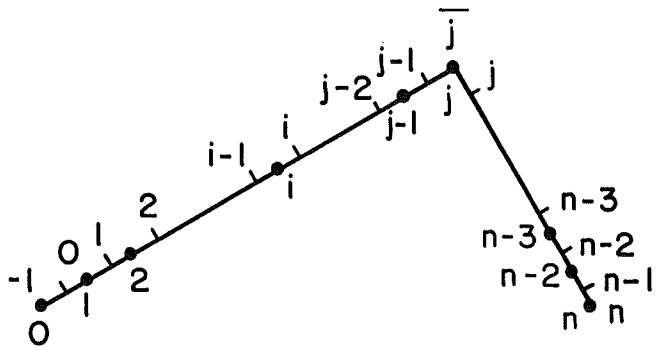

(c) Angle Section-Ends on Integer Stations

FIG. 25 EXAMPLES OF MESH CELLS

12. REFERENCES

1. Yang, C. H., Beedle, L. S., and Johnson, B. G.
   RESIDUAL STRESS AND THE YIELD STRENGTH OF STEEL BEAMS, The Welding Journal, Research Supplement, Vol. 31, April 1952.

2. Huber, A. W., and Beedle, L. S.
   RESIDUAL STRESS AND THE COMPRESSIVE STRENGTH OF STEEL, The Welding Journal, Research Supplement, Vol. 33, No. 12, December 1954.

3. Ketter, R. L.
   THE INFLUENCE OF RESIDUAL STRESSES ON THE STRENGTH OF STRUCTURAL MEMBERS, Welding Research Council Bulletin, No. 44, 1958.

4. Beedle, L. S., and Tall, L.
   BASIC COLUMN STRENGTH, ASCE Proc. Paper 2555, Vol. 86, ST7, July 1960.

5. Fujita, Y.
   INFLUENCE OF RESIDUAL STRESSES ON THE INSTABILITY PROBLEMS, Journal Zosen Kyokai, Japan, Vol. 107, July 1960. (Japanese with English Abstract).

6. Estuar, F. R., and Tall, L.
   EXPERIMENTAL INVESTIGATION OF WELDED BUILT-UP COLUMNS, Welding Journal, Vol. 42, April, 1963.

7. Bleich, F.
   BUCKLING STRENGTH OF METAL STRUCTURES, McGraw-Hill, New York, 1952.

8. Timoshenko, S., and Gere, J. M.
   THEORY OF ELASTIC STABILITY, 2nd Ed., McGraw-Hill, New York, 1961.

9. Lundquist, E. E.
   LOCAL INSTABILITY OF SYMMETRICAL RECTANGULAR TUBES UNDER AXIAL COMPRESSION, NACE TN 686, 1939.

10. Stowell, E. Z., and Lundquist, E. E.
    LOCAL INSTABILITY OF COLUMNS WITH I-, Z-, CHANNEL- AND RECTANGULAR- TUBE SECTIONS, NACA TN 743, 1939.

11. Chwalla, E.
    REPORTS 2nd INTERNATIONAL CONGRESS, Bridge and Structural Engineer, Vienna, 1928.

12. Ros, M., and Eichinger, A.
    REPORTS 3rd INTERNATIONAL CONGRESS, Bridge and Structural Engineer, Paris, 1932.

13. Hencky, H.
ZUR THEORIE PLASTISCHER DEFORMATIONEN UND DER HIERDURCH IM MATERIAL HERVORGE REFENEN NACH SPANNUNGEN, Z. Angew. Math and Mech., Vol. 4, 1924.

14. Reuss, A.
BERUCKSICHTIGUNG DER ELASTISCHEN FORMANDERUNG IN DER PLASTIZITATSTHEORIE, Z. Agew. Math and Mech., Vol. 10, 1930.

15. Bijlaard, P. P.
THEORY OF THE PLASTIC STABILITY OF THIN PLATES, Pub. Int. Assoc., Bridge and Structural Engrg., Zurich, Vol. 6, 1940-41.

16. Bijlaard, P. P.
SOME CONTRIBUTIONS TO THE THEORY OF ELASTIC AND PLASTIC STABILITY, Pub. Int. Bridge and Structural Eng., Zurich, Vol. 8, 1947.

17. Bijlaard, P. P.
THEORY AND TESTS ON THE PLASTIC STABILITY OF PLATES AND SHELLS, Jour. Aero. Sci., Vol. 16, No. 9, September 1949.

18. Bijlaard, P. P.
A THEORY OF PLASTIC STABILITY AND ITS APPLICATION TO THIN PLATES OF STRUCTURAL STEEL, Proc. Royal Netherlands Academy of Sci., Amsterdam, Vol. 41, No. 7, 1938.

19. Ilyushin, A. A.
THE ELASTO-PLASTIC STABILITY OF PLATES, NACA TM 1188, 1947.

20. Stowell, E. Z.
A UNIFIED THEORY OF PLASTIC BUCKLING OF COLUMNS AND PLATES, NACA Rep. 898, 1948.

21. Handelman, G. H., and Prager, W.
PLASTIC BUCKLING OF A RECTANGULAR PLATE UNDER EDGE THRUSTS, NACA Rep. 946, 1949.

22. Pearson, C. E.
BIFURCATION CRITERION AND PLASTIC BUCKLING OF PLATES AND COLUMNS, Jour. Aero., Sci., Vol. 17, No. 7, July 1950.

23. Drucker, D. C.
A DISCUSSION OF THE THEORIES OF PLASTICITY, Jour. of Aero. Sci., Vol. 16, No. 9, September 1949.

24. Bijlaard, P. P.
ON THE PLASTIC BUCKLING OF PLATES ACCORDING TO THE FLOW THEORY, Jour. of Aero. Sci., Vol. 17, No. 12, December 1950.

25. Onat, E. T., and Drucker, D. C.
INELASTIC INSTABILITY AND INCREMENTAL THEORIES OF PLASTICITY, Jour. Aero. Sci., Vol. 20, No. 3, March 1953.

26. Bijlaard, P. P.
ON THEORIES OF PLASTICITY AND THE PLASTIC STABILITY OF CRUCIFORM SECTIONS, Jour., Aero. Sci., Vol. 20, No. 11, November 1963.

27. Bijlaard, P.P.
DISCUSSION TO "INELASTIC BUCKLING IN STEEL", by Haaijer and Thurlimann, Trans. ASCE, Vol. 125, Part I, 1960.

28. Pride, R. A., Heimerl, G. J.
PLASTIC BUCKLING OF SIMPLY SUPPORTED COMPRESSED PLATES, NACA TN 1817, 1949.

29. Ueda, Y.
ELASTIC, ELASTIC-PLASTIC AND PLASTIC BUCKLING OF PLATES WITH RESIDUAL STRESSES, Ph. D. Dissertation, Lehigh University, 1962.

30. Gerard, G., and Becker, H.
HANDBOOK OF STRUCTURAL STABILITY, PART I, NACA TN 3781, 1957.

31. Haaijer, G., and Thurlimann, B.
INELASTIC BUCKLING IN STEEL, Trans. ASCE, Vol. 125, Part I, 1960.

32. Yoshiki, M., Fujita, Y., and Kawai, T.
INFLUENCE OF RESIDUAL STRESSES ON THE BUCKLING OF PLATES, Jour. Zosen Kyokai, Japan, Vol. 107, 1960. (Japanese with English Abstract).

33. Nageraja Rao, N. R., and Tall, L.
RESIDUAL STRESSES IN WELDED PLATES, The Welding Journal, Vol. 40, October 1961.

34. Nageraja Rao, N. R., Estuar, F. R., and Tall, L.
RESIDUAL STRESSES IN WELDED SHAPES, Welding Journal, Vol. 43, July, 1964.

35. Odar, E., Nishino, F., and Tall L.
RESIDUAL STRESSES IN T-1 CONSTRUCTIONAL ALLOY STEEL PLATES, Fritz Laboratory Report No. 290.4, Lehigh University, 1964 to be published in Welding Journal.

36. Richardson. L. F.
THE APPROXIMATE ARITHMETICAL SOLUTION BY FINITE DIFFERENCES OF PHYSICAL PROBLEMS INVOLVING DIFFERENTIAL EQUATIONS WITH AN APPLICATION TO THE STRESSES IN A MASONRY DAM, Phil. Trans. Royal Soc., London, Vol. 210,1911.

37. Collatz, L.
EIGENWERT PROBLEME UND IHRE NUMERISHE BEHANDLUNG, Chelsea Publishing Co., New York, 1948.

38. Salvadori, M. G.
NUMERICAL COMPUTATIONS OF BUCKLING LOADS BY FINITE DIFFERENCES, Trans. ASCE, Vol. 116, 1951.

39. Salvadori, M. G., and Baron, M. L.
NUMERICAL METHODS IN ENGINEERING, Prentice-Hall, Englewood Cliffs, New Jersey, 1952.

40. Jordan, C.
CALCULUS OF FINITE DIFFERENCES, 2nd Ed., Chelsea Publishing Co., New York, 1950.

41. Bodewig, E.
MATRIX CALCULUS, 2nd Ed., North Holland Publishing Co., Amsterdam, Holland, 1959.

42. Faddeeva, V. N.
COMPUTATIONAL METHODS OF LINEAR ALGEBRA, Dover Publications Inc., New York, 1959.

43. Crandall, S. H.
ENGINEERING ANALYSIS, McGraw-Hill Book Co., Inc., New York, 1956.

44. Odar, E., Nishino, F., and Tall, L.
RESIDUAL STRESSES IN ROLLED HEAT-TREATED T-1 STEEL SHAPES, Fritz Laboratory Report No. 290.5, Lehigh University, 1965.

45. Nishino, F.
BUCKLING STRENGTH OF COLUMNS AND THEIR COMPONENT PLATES, Ph. D. Dissertation, Lehigh University, 1964.

46. Nishino, F., Ueda, Y., and Tall, L.
EXPERIMENTAL INVESTIGATION OF THE BUCKLING OF PLATES WITH RESIDUAL STRESSES, Fritz Laboratory Report 290.3, Lehigh University, April, 1966.

47. Hu, P. C., Lundquist, E. E. and Batdorf, S. B.
EFFECT OF SMALL DEVIATIONS FROM FLATNESS ON EFFECTIVE WIDTH AND BUCKLING OF PLATES IN COMPRESSION, NACA TN 1124, 1946.

48. Nishino, F. and Tall, L.
RESIDUAL STRESS AND BUCKLING STRENGTH OF THIN-WALLED COLUMNS, Fritz Laboratory Report 290.7, Lehigh University, in preparation.